Relativistic description of the deuteron and of processes in which it participates in a covariant approach in light-cone variables

M. A. Braun
Leningrad State University, Leningrad

M. V. Tokarev
V. I. Lenin State University, Tashkent

Fiz. Elem. Chastits At. Yadra **22**, 1237–1291 (November–December 1991)

A relativistic description of the deuteron and of processes in which it participates is presented in the framework of a covariant approach in light-cone variables. The *dpn* vertex function with one of the nucleons on the mass shell is taken as the relativistic wave function. It is shown that all amplitudes of interaction with participation of the deuteron can be expressed in terms of it. A scheme of relativization different from the usual one is proposed, and a relativistic wave function that describes the statistical properties of the deuteron and has the well-known wave function as nonrelativistic limit is constructed. The basic importance of the choice of the frame of reference for describing processes in which the deuteron participates is demonstrated. The constructed wave functions are used to describe electromagnetic processes ($ed \to ed$, $ed \to eX$) and processes with strong interaction ($pd \to hX$, $dA \to pX$) with the participation of a polarized (vector and tensor) deuteron and unpolarized deuteron. Calculations of characteristics of the processes (form factors, cross sections, structure functions, etc.) are compared with available experimental data. Predictions are made for some processes ($\vec{pd} \to \pi^+ X$, $\vec{ed} \to ed$, $\vec{ed} \to eX$), the experimental verification of which is of interest both for the development of the relativistic theory of nuclear systems and for the search for new effects due to the quark–gluon structure of hadrons in nuclei.

INTRODUCTION

From the point of view of quantum chromodynamics (QCD), the deuteron is an extremely complicated system, consisting of at least six valence quarks with the possible addition of sea quarks and gluons. At the same time, nonrelativistic physics successfully describes the deuteron as a particle made up of a proton and a neutron. The transition between these descriptions and the identification associated with it of a manifestation of quark degrees of freedom in the deuteron require study of the nucleon wave functions of the deuteron in the relativistic domain. The arrival at the QCD level of description can then be accurately recognized in the deviations of the properties of the real deuteron from the predictions in terms of a nucleon wave function. This explains the great interest shown in recent years in relativization of the description of the deuteron, regarded as a bound state of nucleons. Anticipating, we note that all authors who have worked in this direction have been united in one thing—up to energies of the order of several giga-electron-volts, the existing experimental data fit in the nucleon picture of deuteron structure and do not require a radical transition to a quark level of description, and they do not even require lesser modifications such as allowance for the deformability of nucleons.

The relativistic description of bound states of two particles is an old and complicated problem. In this review, it is not our aim to reflect all the varied, sometimes very interesting approaches in the framework of relativistic quantum field theory or scattering theory.[1–16] Here, we shall restrict ourselves to a brief discussion of the directions that have a historical or direct relation to the method we propose. Conceptually, the most general and simple approach is the traditional one based on the Bethe–Salpeter (BS) equation and wave function

$$F_{\mathrm{BS}}(x_1,x_2) = \langle 0 | T\{\psi_p(x_1)\psi_n(x_2)\} | \Psi \rangle, \qquad (1)$$

where $\psi_{p(n)}$ are the operators of the proton (respectively, neutron) field, and Ψ is the studied bound state (deuteron).[1] For a spherically symmetric spinless deuteron, the BS wave function depends on two variables: the relative separation $|\mathbf{x}_1 - \mathbf{x}_2|$ and the relative time $x_{10} - x_{20}$. From the point of view of the Feynman rules, it corresponds to a *dpn* vertex function in which both nucleons are off the mass shell and have variable "virtualities." The presence of the two variables in the BS function makes calculations with it extremely difficult even with the simplest types of relativistic interaction, and it is also difficult to compare it with the well-studied nonrelativistic wave functions of the deuteron, which depend only on a single variable $(\mathbf{x}_1 - \mathbf{x}_2)$. In the BS equation, the relativistic interaction is known only in the form of a perturbation-theory series and is not characterized by any distinguished qualities as a function of its variables (for example, a locality property which holds such as holes for the nonrelativistic potential). This opens up wide possibilities for the construction of other deuteron wave functions that are a restriction of the BS wave function to a certain, in general, arbitrarily chosen subspace of values of x_1 and x_2 or the corresponding conjugate momenta k_1 and k_2. The general scheme of such a construction is very simple. Suppose the

 0090-4759/91/060601-27$04.00

two-particle Green's function of the proton and neutron in the original space is G. It satisfies the BS equation

$$G=G_0+G_0KG, \tag{2}$$

where K is the relativistic interaction, and all symbols denote operators acting on the space x_1x_2 or k_1k_2. The formal solution of (2) is obviously

$$G=(G_0^{-1}-K)^{-1}. \tag{3}$$

We now consider the restriction of G to some arbitrary subspace Ω of the original space of coordinates or momenta: $G_\Omega \equiv g$. Obviously, the inverse operator g^{-1} is not equal to G^{-1}, but it can be found if G is known. We represent g^{-1} in a form analogous to (3):

$$g=(g_0^{-1}-k)^{-1}, \tag{4}$$

where g_0 is an arbitrarily chosen (as simply as possible) operator on Ω that can be naturally interpreted as the Green's function on Ω without allowance for the interaction. The expression (4) then serves as a definition of the interaction k in the subspace Ω. A consequence of (4) is a BS equation in Ω:

$$g=g_0+g_0kg. \tag{5}$$

Regarding (5) as a function of the square P^2 of the total momentum and taking the residue at the point M^2, where M is the deuteron mass, we find a BS equation for a function f that is the restriction of F_{BS} to the subspace Ω:

$$f=g_0kf. \tag{6}$$

In principle, this equation is not worse than the original one. The potential k can be determined in perturbation theory from the original K, as described above.

A classical example of the use of this scheme is the quasipotential method, which realizes a restriction of the space x_1x_2 to the space of equal times with $x_{10}=x_{20}$ (Ref. 3). Another obvious possibility is to fix the virtuality of one of the nucleons [for this, of course, it is necessary to consider (2) in the momentum space and go over from G to the function $T=G_0^{-1}GG_0^{-1}$]. Incidentally, it is clear that there is here an infinite set of possibilities; for one can regard as given any combinations of coordinates or momenta of the particles and obtain equations for the restricted wave functions. In recent years, a choice that has become very popular is restriction to the subspace $x_{1+}-x_{2+}$, where $x_\pm$ are light-cone variables: $x_\pm=(1/\sqrt{2})\times(x_0\pm x_z)$. In this case, an equation for f can also be obtained independently of the BS equation, from a direct consideration of the graphs for the "old" perturbation theory.[6] The wave function obtained in this way depends on two variables [$(x_{1-}-x_{2-})$ and $|x_{1\perp}-x_{2\perp}|^2$] and in this respect is not better than the original F_{BS}. Nevertheless, in some special cases one can go over to wave functions that depend on only one variable. This is the case with the quasipotential wave functions, in which there remains only the dependence on $|x_1-x_2|$. Wave functions that depend on only one variable are also obtained by relativistically invariant restrictions in the space of virtualities of the type $\alpha k_1^2+\beta k_2^2=m^2$.

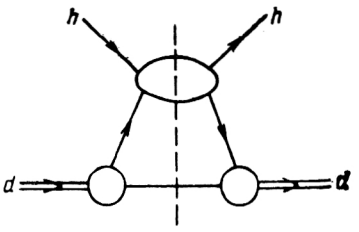

FIG. 1. Absorptive part of the amplitude for forward scattering of a particle (h) by the deuteron (d) in the impulse approximation.

However, the construction of a relativistically invariant wave function that depends on only one variable does not yet by itself solve all the problems associated with describing the deuteron. It would be sufficient to determine the deuteron binding energy for a given interaction (i.e., given k). However, k is actually unknown, like K on the complete space, and it is much more sensible to take the binding energy from experiment. The main task is to correlate experimental facts on the interaction of the deuteron with other particles or fields. In this perspective, the transition to restricted wave functions gives little; for we know how to express any amplitude with participation of the deuteron in terms of the original BS function F_{BS}, but after the restriction to f this simple connection is lost and it is actually necessary to reconstruct the entire theory of scattering by the deuteron. It can be seen that the task is to construct a wave function that depends on a single variable and in terms of which a scattering amplitude with participation of the deuteron can be naturally expressed. The review of studies in the present paper is devoted to this problem.

As the deuteron wave function, we consider the *dpn* vertex function with one of the nucleons on the mass shell. Using the technique of light-cone variables, proposed originally for calculations in the so-called covariant parton model,[17] we show that all amplitudes of interactions with participation of the deuteron can be expressed in terms of a wave function in these variables.

The circumstance that the *dpn* vertex function with nucleon spectator on the mass shell appears naturally in an analysis of cross sections of interactions with the deuteron is in general rather trivial and well known. Indeed, the amplitude of an interaction with a deuteron corresponds in the impulse approximation to allowance for the graph shown in Fig. 1, in which the deuteron is represented by the double line. The transition to the cross section corresponds to taking the absorptive part of the forward scattering amplitude (graphically, the cutting of the diagram is shown in Fig. 1 by the broken line). The spectator nucleon is then taken onto the mass shell, and both of the ingoing *dpn* vertices are functions of only the virtuality of the active nucleon. Much less trivial, and new, is the fact that not only the absorptive parts but also the amplitudes themselves, in particular the form factors, can be expressed in terms of the *dpn* vertex with one of the nucleons on the mass shell. It is this circumstance that allows us to regard such a vertex as a fully valid relativistic wave function of

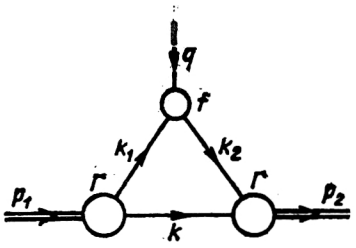

FIG. 2. Deuteron form factor in the impulse approximation.

the deuteron, and also to construct for it a relativistic wave equation. This assertion will be demonstrated below in Secs. 1–3 for the example of the scalar deuteron. The remainder of the review is devoted to allowance for spins and actual applications.

We should mention that in addition to the approaches mentioned above there have been some other approaches in the literature to relativization of the deuteron wave function that lead to wave functions that depend on a single variable; these are based on various poorly justified approximations. Thus, in the studies of Strikman and Frankfurt (see the reviews of Refs. 12–14) the relative variables x and $k_\perp$ in the wave function $\psi(x = k_+/p_+, k_\perp)$, which is defined on the hypersurface $x_{1+} - x_{2+} = 0$, are combined without proper justification into a single argument (see the criticism in Ref. 10). In the studies of Gross *et al.*,[5,18–21] in which essentially the same wave function is used as in our studies, but in different variables and, as a consequence, with different results, the equation for the wave function and the expressions for the form factors are obtained in an approximation in which nonvanishing contributions from all poles of the integrand apart from the contribution from the spectator nucleon are ignored. In our studies, no such approximations are made, and the results have a rigorous nature in the framework of the adopted representation of the deuteron as a composite of two nucleons.

1. WAVE FUNCTION AND FORM FACTORS OF THE DEUTERON

In this section, we shall demonstrate that the *dpn* vertex function with one nucleon off the mass shell and expressed in light-cone variables plays the role of a wave function in a calculation of the deuteron form factor in the impulse approximation.[22] So as not to obscure key points in the derivation, in this and the following two sections we shall consider the model case of spinless particles (nucleons and the deuteron). Allowance for the spins does not change the fundamental conclusions and will be done fully later.

In the impulse approximation, the deuteron form factor (electromagnetic or baryon) corresponds to the diagram shown in Fig. 2. Explicitly, it is represented as an integral over the momentum of the virtual spectator nucleon

$$F_\mu(q) = \int (d^4k/(2\pi)^4 i) f_\mu(q,k)\Gamma(k^2,k_1^2)\Gamma(k^2,k_2^2) \times (m^2-k^2)^{-1}(m^2-k_1^2)^{-1}(m^2-k_2^2)^{-1}. \quad (7)$$

Here, f_μ is the form factor of the (scalar) nucleon, Γ are *dpn* vertex functions with both nucleons off the mass shell, and m is the nucleon mass. We shall show that if light-cone variables are used, F_μ can be expressed in terms of vertices Γ with the spectator nucleon on the mass shell.

We introduce the components $k_\pm$ by the relation

$$k_\pm = (k_0 \pm k_z)/\sqrt{2}. \quad (8)$$

We shall consider the form factor in the region of spacelike q and assume that q is purely transverse. We assume that the vector $p = \frac{1}{2}(p_1 + p_2)$, which is orthogonal to q, is purely longitudinal. The nucleon form factor f_μ has the usual vector structure

$$f_\mu(q,k) = (k_{1\mu} + k_{2\mu}) f(q^2,k_1^2,k_2^2). \quad (9)$$

We consider the integration over the variable k_- in the integral (7). In the plane of the complex variable k_-, singularities of the integrand arise from singularities with respect to the three virtualities k^2, k_1^2, and k_2^2, which are situated in regions in which there exist corresponding intermediate states: $k^2 \geqslant m^2$, $k_1^2 \geqslant m^2$, $k_2^2 \geqslant m^2$. Some of these singularities (pole singularities) are separated explicitly in the form of propagators, and the remainder are associated with the vertex parts Γ and the form factor f. In the variable k_-, the singularities that arise from k^2, k_1^2, and k_2^2 lie, respectively, in the regions

$$k_- \geqslant (m_\perp^2 - i0)/2k_+,$$

$$p_{1,2-} - k_- \geqslant (m_{1,2\perp}^2 - i0)/2(p_{1,2+} - k_+), \quad (10)$$

where $m_\perp^2 = m^2 - k_\perp^2$, $m_{11}^2 = m^2 - k_{1\perp}^2$, and $m_{2\perp}^2 = m^2 - k_{2\perp}^2$. Since $p_1 = p - q/2$, $p_2 = p + q/2$ and q is purely transverse, $p_{1\pm} - k_\pm = p_{2\pm} - k_\pm = p_\pm - k_\pm$ and the same in the second pair of inequalities in (10). If the integral over k_- is to be nonzero, the singularities in k_- must lie on opposite sides of the real axis. It then follows from (10) that the signs of k_+ and $p_+ - k_+$ must be the same. Since, as we are assuming, p_+ is positive, this gives a restriction on the range of variation of k_+:

$$0 \leqslant k_+ \leqslant p_+ - k_+. \quad (11)$$

Closing the contour of integration around the singularities with respect to k_- in the lower half-plane, and retaining from these singularities only the contribution of the nucleon pole in accordance with the impulse approximation, we find for the + component in (7)

$$F_+(q) = \int_0^{p_+} \frac{dk_+ d^2k_\perp}{2k_+(2\pi)^3} 2k_+ f(k_1^2,k_2^2)\Gamma(m^2,k_1^2) \times \Gamma(m^2,k_2^2)(m^2-k_1^2)^{-1}(m^2-k_2^2)^{-1}, \quad (12)$$

where k_1^2 and k_2^2 are expressed in terms of k_+ and k_- by means of the relations

$$k_1 = p_1 - k, \quad k_2 = p_2 - k, \quad k_- = m_\perp^2/2k_+. \quad (13)$$

Equation (12) can also be written in the form

$$F_+(q)=\int \frac{d^4k}{(2\pi)^4 i}\,2\pi i\delta(m^2-k^2)\theta(k_0)\theta(p_+ - k_+)2k_+ f(k_1^2,k_2^2)\Gamma(m^2,k_1^2)\Gamma(m^2,k_2^2)\times(m^2-k_1^2)^{-1}(m^2-k_2^2)^{-1}. \quad (14)$$

It can be seen that the transition from (7) to (14) corresponds to taking the spectator nucleon onto the mass shell together with the restriction on the region of integration with respect to the variable k_+. The noninvariant nature of this restriction is due to a special choice of the frame of reference, in which $g_+ = 0$ (we also required $q_- = 0$, but this is not necessary; see Sec. 3). We also recall in connection with the derivation of (12) that because light-cone variables are used the points $k_\pm = 0$ are singular, and it is necessary to consider the existence of the integrals. In our case, this circumstance dictates the choice of the + component for the form factor F_μ. For the − component, the analogous procedures are invalid and lead to divergences at small k_+. Separating the scalar part of the form factor F_μ by the relation

$$F_\mu = 2p_\mu F(q^2) \quad (15)$$

and introducing the scaling variable $x = k_+/p_+$, we write the final expression for the form factor as

$$F(q^2)=\int_0^1 \frac{dx}{2x}\int \frac{d^2k_\perp}{(2\pi)^3}\,x f(q^2,k_1^2,k_2^2)\varphi(k_1^2)\varphi(k_2^2), \quad (16)$$

where we have introduced the function

$$\varphi(k^2)=\Gamma(m^2,k^2)(m^2-k^2)^{-1} \quad (17)$$

and the variables k_1^2 and k_2^2 are expressed in terms of x and $k_\perp$ by formulas that follow from (13):

$$k_{1(2)}^2=(1-x)M^2+(1-1/x)m^2 + (k_\perp+(-)xq_\perp/2)^2/x. \quad (18)$$

The expression (16) has been obtained for $q^2 < 0$. The transition to $q^2 > 0$ can be made by analytic continuation of (16) with respect to $q^2 = q_\perp^2$.

Thus, we have indeed succeeded in expressing the deuteron form factor in terms of *dpn* vertex functions with the spectator nucleon on the mass shell. As can be seen from (16), or even more clearly from (14), the functions $\varphi(k^2)$ play the part of deuteron wave functions, entering the form factor in the same manner that nonrelativistic wave functions enter a nonrelativistic form factor. Only the choice of the arguments and the region of integration are nontrivial.

In principle, the expression (16) takes into account the dependence of the nucleon form factor f on the virtuality of the nucleon, i.e., the change of the electromagnetic (or baryon) properties of a nucleon in a deuteron compared with a free nucleon. In practice, the wave functions $\varphi(k_1^2)$ decrease fairly rapidly with increasing $m^2 - k_1^2$, so that the integration in (16) is over a comparatively narrow region near $k_{1(2)}^2 = m^2$. This enables us to ignore the dependence of f on the departure from the mass shell, which is, in fact, natural in the philosophy of the impulse approximation. Then (16) can be rewritten in the simple form

$$F(q^2)=f(q^2)\int_0^1 \frac{dx}{2x}\int \frac{d^2k_\perp}{(2\pi)^3}\,x\varphi(k_1^2)\varphi(k_2^2). \quad (19)$$

The form-factor normalization condition $F(0) = f(0) = 1$ gives a normalization condition for the wave function φ:

$$\int_0^1 \frac{dx}{2}\int \frac{d^2k_\perp}{(2\pi)^3}\varphi^2(k^2)=1, \quad (20)$$

where in accordance with (18)

$$k^2=(1-x)M^2+(1-1/x)m^2+k_\perp^2/x. \quad (21)$$

This makes it possible to give the function $\varphi/\sqrt{2}$ a probability interpretation—the square of its modulus gives the probability for finding in the relativistic deuteron nucleons with transverse momentum $\pm k_\perp$ and fractions x and $1-x$ of the longitudinal momentum p_+ for the spectator and active nucleon, respectively.

The wave function $\varphi(k^2)$ depends on only one argument, since the variables x and $k_\perp$ are combined in k^2 in accordance with Eq. (21). This is its main advantage compared with the wave functions in light-cone variables that are constructed in Weinberg's technique as Fock components of the neutron state on the hypersurface $x_+ = 0$. However, in contrast to the latter, $\varphi(k^2)$ is not symmetric with respect to the two nucleons, i.e., with respect to the substitution $x \to 1-x$. From the physical point of view, this is not that unusual, since the spectator and the active nucleon play different parts in the observation process. Note that in the approximation in which the dependence of the vertex function on the virtuality is altogether ignored, i.e., $\Gamma(m^2,k^2) \simeq \Gamma(m^2,m^2)$ and the wave function reduces to a pole, $\varphi(k^2) = C(m^2 - k^2)^{-1}$, we find from (21) $\varphi(x,k_\perp) = C(1-x)^{-1}[m_1^2/x(1-x) - M^2]^{-1}$, i.e., apart from the factor $(1-x)^{-1}$ the variables x and $k_\perp$ are combined in the argument $m_1^2/[x(1-x)]$, which is symmetric with respect to the substitution $x \rightleftarrows 1-x$. It was asserted in Refs. 12–14 and 23 that the deuteron wave function in light-cone variables must depend on x and $k_\perp$ precisely through this argument, the assertion being based on the so-called angle condition,[24] which represents the requirement of spherical symmetry for the deuteron S state. This assertion has frequently been criticized.[10] It follows from our arguments that x and $k_\perp$ are combined into the argument $m_1^2/[x(1-x)]$ in the crudest approximation in which the dependence of the vertex function on the virtuality is completely ignored and the wave function reduces to a propagator. At the nonrelativistic level, this corresponds to the zero-range approximation.

In conclusion, we emphasize the utility of the light-cone variables. In the variables k_0, $\mathbf{k}$ the integrand in (7) has, as a function of k_0, six poles from intermediate two-nucleon states, three of which lie below and three above the real axis. In the Breit frame ($\mathbf{p} = 0$, $q_0 = 0$), the poles lie at the points $k_0 = \pm\sqrt{m^2+\mathbf{k}^2}$, $\mathbf{p} - k_0 = \pm[m^2 + (\mathbf{k} \pm \mathbf{q}/2)^2]^{1/2}$. Therefore, in the calculation of the integral (7) it is necessary to take into account not only the

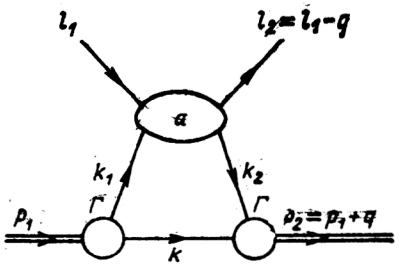

FIG. 3. Amplitude for scattering of a scalar particle (l_1) on the deuteron (d) in the impulse approximation.

pole of the spectator nucleon but also two poles of the active nucleon, which actually correspond to production of nucleon–antinucleon pairs by the external field. As follows from (14), the contribution of these poles actually cancels the part of the contribution from the spectator pole corresponding to the region $k_+ > p_+$ and leads to the appearance of the restriction $k_+ < p_+$ in the exact result. At small q^2, this contribution is small, but its importance grows with increasing q^2, so that it is certainly significant at relativistic q^2. The use of the light-cone variables makes it possible to take into account this contribution automatically and rigorously in the form of the condition $k_+ < p_+$ under the integral sign in (14). As was noted in the Introduction, the approach of Gross's group is well known in the literature.[5,18–21] In it, in the integration in the variables k_0, **k** only the contribution of the spectator pole is taken into account, the remaining poles being ignored. This is equivalent to absence of the restriction $k_+ < p_+$. It is clear that at small q^2 such an approximation gives the same result as our expressions. However, with increasing q^2 a difference arises on account of the condition $k_+ < p_+$, i.e., on account of the contributions, ignored in Refs. 5 and 18–21, from the poles of the active nucleon, even though the wave function used by Gross *et al.* is the same as our function $\varphi(k^2)$. Therefore, despite the identity of the employed wave function, the results of the calculation of the form factors (see Sec. 6) and the equation for the wave function in our studies and in those of Gross *et al.* are different, owing to the use of different variables and, as a consequence, the approximations made by Gross *et al.*

2. SCATTERING AMPLITUDES WITH PARTICIPATION OF A DEUTERON AT HIGH ENERGIES

We shall attempt to extend the results obtained in the previous section for the form factors to more complicated amplitudes involving the deuteron.[25] As we shall see in the case in which the interaction energy is high, arbitrary deuteron interaction amplitudes can be expressed in terms of the wave functions $\varphi(k^2)$ associated with *dpn* vertices with the spectator nucleon on the mass shell.

We consider the amplitude for scattering of an arbitrary scalar particle by a deuteron in the impulse approximation (Fig. 3). Like the form factor, it can be expressed as an integral over the momentum of the virtual spectator:

$$A=\int (d^4k/(2\pi)^4\mathrm{i})a(l_1,k_1,q)\Gamma(k^2,k_2^2) \times\Gamma(k^2,k_1^2)(m^2-k^2)^{-1}(m^2-k_1^2)^{-1}(m^2-k_2^2)^{-1}. \tag{22}$$

The amplitude a describes scattering by the virtual constituent nucleon and is a scalar function of the four variables $s_1=(l_1+k_1)^2, q^2, k_1^2, k_2^2$. The vectors $p=\frac{1}{2}(p_1+p_2)$ and $l=\frac{1}{2}(l_1+l_2)$ are orthogonal to q. We assume that q is purely transverse, and p and l are purely longitudinal.

We again calculate the integral (22) in the light-cone variables and consider the integral with respect to k_-. In the plane of the complex variable k_-, there now appear, in addition to the previous singularities (10) for the form factor, two new singularities, which arise from the right and left cuts of the amplitude a as a function of s_1. In terms of k_{1-}, the singularities at the points $s_1=\mu^2$ and $u_1=\mu^2$ generate the singularities

$$l_-\pm(p_--k_-)=(\mu_\perp^2-\mathrm{i}0)/2[l_+\pm(p_+-k_+)], \tag{23}$$

where $\mu_\perp^2=\mu^2-k_\perp^2$. The appearance of the new singularities (23) will in general change the result obtained in the calculation of the form factor. Even in the region $0\leqslant k_+\leqslant p_+$, the singularity in (23) corresponding to the lower sign may be in the lower half-plane, and it must be added to the pole contribution of the spectator. For $k_+ > p_+$ the integral now does not vanish, since the singularity in (23) corresponding to the upper sign remains in the upper half-plane as long as $k_+\leqslant l_++p_+$. Thus, in the general case the transition from the form factor must also take into account other singularities of the integrand from the amplitude a, and, thus, strict placing of the spectator on the mass shell is impossible.

The situation becomes simpler on the transition to high energies. Suppose that the energy variable $s=(p+l)^2$ for the considered amplitude is large: $s\gg m^2$. We choose the antilaboratory frame of reference relative to the deuteron, in which the deuteron moves rapidly along the z axis, and the momentum l is finite. Then $p_+\sim s/m\gg m$, $p_-\sim m^3/s$, $l_\pm\sim m$. In this frame of reference, we can ignore p_- in (23) compared with l_- and l_+ compared with p_+. Then from (23) we find singularities with respect to k_- at the points

$$l_-\mp k_-=\pm(\mu_\perp^2-\mathrm{i}0)/[2(p_+-k_+)]. \tag{24}$$

The positions of these singularities with respect to the real axis are exactly the same as those already considered for the case of the form factor, namely, outside the region $0\leqslant k_+\leqslant p_+$ they have the same positions as the first of the singularities of (10), and inside this region they lie above the real axis. Therefore, only the indicated range of k_+ values makes a contribution, and the value of the integral with respect to k_- is given by the residue at the pole that derives from the spectator. Introducing again the variable $x=k_+/p_+$, we find, thus, at high energies

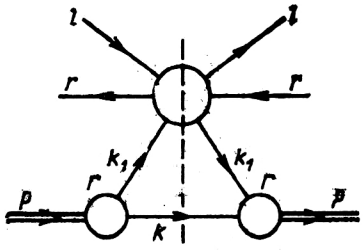

FIG. 4. Impulse approximation for inclusive production of a cumulative particle (r) on the deuteron (d) (direct mechanism).

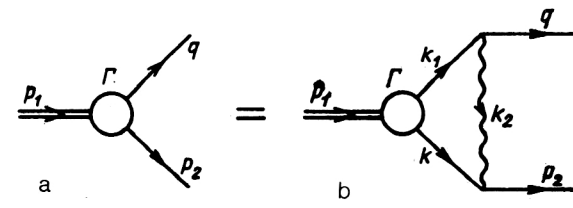

FIG. 5. Bethe–Salpeter equation for the vertex function Γ in the ladder approximation.

$$A=\int \frac{d^2k_\perp}{(2\pi)^3}\int_0^1 \frac{dx}{2x}a(s_1,q^2,k_1^2,k_2^2)\varphi(k_1^2)\varphi(k_2^2). \quad (25)$$

Here, $k_{1(2)}^2$ are given by the previous expressions (18). For scattering by a constituent nucleon, the energy variable s_1 is expressed in terms of x and $k_\perp$ by the relation $s_1 = (l + p - k)^2$, in which it is necessary to assume $k_- = m_\perp^2/2k_+$ and take into account the relative orders of the quantities in the chosen frame of reference. Apart from quantities having relative order m^2/s, we find that $s_1 = 2l(p - k) = (1 - x)s$.

The upshot is that we have succeeded in expressing the amplitude for scattering by the deuteron at high energies in the impulse approximation in terms of the amplitude for scattering by the constituent nucleon and the wave functions $\varphi(k^2)$ associated with the dpn vertex function with the spectator nucleon on the mass shell. Of course, as in the case of the form factor, it is sensible in the spirit of the impulse approximation to ignore the dependence of the amplitude a on the virtualities k_1^2 and k_2^2. Then the amplitude a in (25) depends only on the Feynman variable of integration x. If we introduce the "unintegrated" form factor by

$$p(x,q^2)=\frac{1}{2}\int \frac{d^2k_\perp}{(2\pi)^3}\varphi(k_1^2)\varphi(k_2^2), \quad (26)$$

then we find from (25)

$$A(s,q^2)=\int_0^1 \frac{dx}{x}p(x,q^2)a[(1-x)s,q^2]. \quad (27)$$

At the same time, the form factor itself is expressed in terms of p by

$$F(q^2)=f(q^2)\int_0^1 dxp(x,q^2), \quad (28)$$

and the normalization condition for p is

$$\int_0^1 dxp(x,0)=1. \quad (29)$$

This result can be generalized directly to more complicated interaction amplitudes involving the deuteron at high energies. For example, in connection with inclusive cross sections for particle production on the deuteron, we will be interested in the six-point forward scattering amplitude, which in the impulse approximation corresponds to the diagram in Fig. 4. Its imaginary part gives the inclusive cross section $I_d(s,\alpha,r_\perp)$ for production of particle $r=\{r_+ + \alpha p_+, r_\perp\}$ in a collision of an incident particle (momentum l) with the deuteron (momentum p) at energy $\sqrt{s}$ in the center-of-mass system. The operation of taking of the imaginary part immediately places the spectator nucleon on the mass shell. We perform the remaining three-dimensional integration in the variables x and k_+. In the integrand we have the inclusive cross section $I_N(s_2,z,r_1')$ for production of a particle on the virtual active nucleon. The virtuality k_1^2 is expressed in terms of x and $k_\perp$ by the previous formula (21). As before, $s_1 = (1 - x)s$. The variable $u = (k_1 - r)^2$ is related to the variables of integration by $u = (1 - z)m^2 + (1 - 1/z)\mu^2 + (r_\perp - zk_\perp)^2/z$, where $z = r_+/k_{1+} \leqslant 1$, and μ is the mass of the detected particle. From this we conclude that $z = \alpha/(1-x) \leqslant 1$ and $r_\perp' = r_\perp - zk_\perp$. If we also ignore the dependence of the inclusive cross section I_N on the virtuality of the nucleon, then we finally obtain

$$I_d(s,\alpha,r_\perp)=\int_0^{1-\alpha}\frac{dx}{2x}\int\frac{d^2k_\perp}{(2\pi)^3} \times I_N[(1-x)s,\alpha/(1-x),r_\perp']\varphi^2(k_1^2), \quad (30)$$

with k_1^2 given by (21), and

$$r_\perp'=r_\perp-\alpha/(1-x)k_\perp. \quad (31)$$

3. EQUATION FOR THE WAVE FUNCTION. NONRELATIVISTIC LIMIT

As we have established, the main quantities that describe the interaction with a deuteron can be expressed in terms of the wave function φ, which is the dpn vertex function with one virtual nucleon with its propagator included. In order to raise φ to the status of a true wave function, we construct for it an equation that, in principle, also determines the deuteron binding energy.[22] The BS equation for the vertex $\Gamma(q^2,p_2^2)$ in the ladder approximation and neglect of self-masses is shown graphically in Fig. 5. The wavy line corresponds to exchange of a meson or several mesons, i.e., to the relativistic interaction in the ladder approximation $V(k_2)$, $k_2 = p_2 - k$. Explicitly,

$$\Gamma(q^2,p_2^2)=\int\frac{d^4k}{(2\pi)^4 i}V(k_2)\Gamma(k^2,k_1^2) \times(m^2-k^2)^{-1}(m^2-k_1^2)^{-1}. \quad (32)$$

We shall calculate the right-hand side of Eq. (32), i.e., the diagram of Fig. 5b, by the same methods as the form factor, taking one of the external nucleons to be physical, $p_2^2 = m^2$, and the other virtual with spacelike momentum $q^2 < 0$.

We use the light-cone variables $k_\pm$, $k_\perp$. The calculations effectively repeat the case of the form factor, except that the squares of the momenta p_1 and p_2 are now different: $p_1^2 = M^2$, while $p_2^2 = m^2$. We shall assume that $q_+ = 0$, and that the deuteron momentum is purely longitudinal, $p_{1\perp} = 0$. Then $p_{2+} = p_{1+}$ and $k_{2+} = k_{1+}$. We shall describe the singularities with respect to k_- by the previous conditions (10), and the disposition of the singularities corresponding to the second condition (10) will again be the same, being determined by the sign of $p_{1+} - k_+$. The upshot is that we obtain the previous result, namely, the integral is nonvanishing only in the region $0 \leqslant k_+ \leqslant p_{1+}$ and can be calculated by closing the contour of integration in the k_- plane around the pole at the point $k^2 = m^2$. Introducing $x = k_+/p_+$, we find in complete analogy with (14) or (16)

$$(m^2 - q^2)\varphi(q^2) = \int_0^1 \frac{dx}{2x} \int \frac{d^2k_\perp}{(2\pi)^3} V(k_2^2)\varphi(k_1^2). \tag{33}$$

Here, we have gone over to the function $\varphi(k^2) = \Gamma(m^2,k^2)(m^2 - k^2)^{-1}$. Expressions for $k_{1,2}^2$ can be readily obtained by the substitution $k_- = m_\perp^2/2k_+$. These expressions generalize (18) to the case of unequal masses:

$$\left.\begin{aligned} k_1^2 &= (1-x)M^2 + (1-1/x)m^2 + k_\perp^2/x; \\ k_2^2 &= (2-x-1/x)m^2 + (k_\perp - xq_\perp)^2/x. \end{aligned}\right\} \tag{34}$$

Equation (33) is obtained in the distinguished frame of reference fixed by the condition $q_{1+} = 0$. Therefore, it does not have a relativistically invariant form. If we return to the variable 4-momentum k, the equation can be written in a form analogous to (14):

$$(m^2 - q^2)\varphi(q^2) = \int \frac{d^4k}{(2\pi)^4 i} 2\pi i\delta(m^2 - k^2) \times \theta(k_0)\theta(p_{1+} - k_+) V(k_2^2)\varphi(k_1^2), \tag{35}$$

where $k_1 = p_1 - k$, $k_2 = p_2 - k$. As in (14), the right-hand side of (35) differs from the pure pole contribution of the spectator nucleon only in the restriction on the region of integration with respect to k_+, which has a manifestly noninvariant nature. Actually, Eq. (35) has a restricted invariance with respect to Lorentz transformations along the z axis and rotations in the transverse plane. However, this circumstance in no way affects the complete relativistic invariance of the function $\varphi(q^2)$, Using it, we can readily represent Eq. (33) of (35) in a manifestly relativistically invariant form. Introducing an integration over the virtualities k_1^2 and k_2^2, we rewrite (33) in the form

$$(m^2 - q^2)\varphi(q^2) = \int dk_1^2 K(q^2,k_1^2)\varphi(k_1^2), \tag{36}$$

where the kernel K is determined by

$$K(q^2,k_1^2) = \int dk_2^2 \int_0^1 \frac{dx}{2x} \int \frac{d^2k_\perp}{(2\pi)^3} V(k_2^2) \times \delta[k_1^2 - k_1^2(x,k_\perp)]\delta[k_2^2 - k_2^2(x,k_\perp)] \tag{37}$$

and the functions $k_1^2(x, k_\perp)$ and $k_2^2(x, k_\perp)$ are the right-hand sides of the relations (34). In the form (36), the equation for $\varphi(k^2)$ is obviously relativistically invariant and one-dimensional.

A question of practical importance is the relation of $\varphi(k^2)$ to the nonrelativistic wave function and the associated question of the nonrelativistic limit of Eq. (33). To go over to the nonrelativistic limit, it is convenient, using the invariance of the equation with respect to Lorentz transformations along the z axis, to go over in (35) to the deuteron rest frame: $p_{1+} = p_{1-} = M$, $p_{1\perp} = 0$. Since then $p_2 = q$, in this frame

$$\left.\begin{aligned} q^2 &= M^2 + m^2 - 2M\sqrt{m^2 + \mathbf{q}^2}; \\ k_1^2 &= M^2 + m^2 - 2M\sqrt{m^2 + \mathbf{k}^2}; \\ k_2^2 &= 2m^2 - 2\sqrt{m^2 + \mathbf{q}^2}\sqrt{m^2 + \mathbf{k}^2} + 2(\mathbf{kq}). \end{aligned}\right\} \tag{38}$$

Therefore, the wave functions $\varphi(q^2)$ and $\varphi(k_1^2)$ in (35) can be regarded as functions of $\mathbf{q}^2$ and $\mathbf{k}^2$, respectively. Integration over k_0 then gives the following equation in the deuteron rest frame:

$$(2\sqrt{m^2 + \mathbf{q}^2} - M)\varphi(\mathbf{q}^2) = \frac{1}{M} \int \frac{d^3k}{2(2\pi)^3\sqrt{m^2 + \mathbf{k}^2}} V(k_2^2)\varphi(\mathbf{k}^2) \times \theta(M - \sqrt{m^2 + \mathbf{k}^2} - k_z). \tag{39}$$

This equation is similar to a Schrödinger equation with relativistic kinematics or a quasipotential equation.[3] The main difference is the presence of the θ function, which bounds the region of integration with respect to k_z by quantities of order m on the side of positive values.

The passage to the nonrelativistic limit can now be made easily. We set $M = 2m - \varepsilon$ and take the limit as $m \to \infty$ for fixed $\mathbf{q}$, $\mathbf{k}$, and ε. Then it can be seen that (39) goes over into an ordinary Schrödinger equation with potential in the momentum space equal to $V(-\mathbf{k}^2)/4m^2$. At the same time, the restriction on the region of integration with resepct to k_z disappears. A similar transition can be made in the normalization condition (20). In the deuteron rest frame, the variable $x = k_+/p_+$ becomes $(\sqrt{m^2 + \mathbf{k}^2} - k_z)/M$ and in the nonrelativistic limit gives m/M. After this, we obtain the usual nonrelativistic normalization condition in the momentum space for the wave function $\varphi(\mathbf{k}^2)/\sqrt{2M}$. The factor $1/\sqrt{2M}$ is obviously related to the transition from the relativistic normalization of the states to a nonrelativistic one.

4. ELECTROMAGNETIC DEUTERON FORM FACTORS: ALLOWANCE FOR SPINS

Actual calculations require a transition to real deuterons and nucleons with spin.[25–27] Allowance for spin does

not change the fundamental aspects of the method, since the spin factors do not destroy the analytic properties of the amplitudes as functions of k_-. The final conclusion can be reduced to formulas of the type (14) or (25), namely, the spectator nucleon is taken onto the mass shell, and there appears the restriction $k_+ < p_+$, the significance of which is transparent in the infinite-momentum frame of the deuteron—it suppresses the component with negative energy. In this connection, the expressions for the various processes in our approach are similar to the analogous expressions in Gross's approach, in which the spectator nucleon is also on the mass shell. The difference from the approach of Gross *et al.* reduces to the restriction on the region of integration with respect to k_+, which arises, as was explained in Sec. 1, when complete allowance is made for all the poles of the integrand. A consistent theory should begin with the construction of the wave function of the deuteron and determination of its binding energy. The constructed wave function could then be used to study interactions of the deuteron. In principle, such a program can be realized. For the deuteron with spin, one can construct a wave equation by following the method discussed in Sec. 3. The form of this equation is the same as that of the equations proposed in Ref. 5, which must be considered in the frame with $q_+ = 0$, and restrictions must be introduced on the region of integration with respect to the momentum of the real spectator nucleon: $k_+ < p_+$. For a given *pn* potential, one could seek from this the wave function and the binding energy. However, in our opinion, such a program is not satisfactory because the *pn* potential is poorly known in the relativistic region. Therefore, it appears more constructive to use a semiphenomenological approach in which the binding energy of the deuteron and its wave function are chosen in accordance with experimental data, in particular, on the basis of the well-known nonrelativistic deuteron wave functions. The wave function obtained in this manner can then be used to describe interaction processes involving the deuteron. Such an approach was used in Refs. 25–30.

When spins are taken into account, the deuteron wave function ψ_α, defined as the *dpn* vertex with one of the nucleons (p or n) on the mass shell and the propagators of the active nucleon included, is a vector with respect to the deuteron spin and a 4×4 matrix with respect to the nucleon spin indices. It is convenient to describe the active nucleon by the charge-conjugate field. Then the structure of the wave function ψ_α is the same as for the standard vector vertex of a spinor nucleon with the initial or final nucleon on the mass shell:

$$\psi_\alpha(k)=k_\alpha[u_1+u_2(m+\hat{k})]+\gamma_\alpha[u_3+u_4(m+\hat{k})]. \tag{40}$$

Here, k is the momentum of the active (initial) nucleon; $u_i = u_i(k^2)$ are the scalar components of the deuteron wave function. It can be seen that the relativistic deuteron is described by four scalar functions, in contrast to the nonrelativistic deuteron, which is described by two functions: the S and D waves. The connection between the functions u_i and the nonrelativistic wave functions will be discussed in the following section when we determine the actual form of u_i, since the precise correspondence takes into account the normalization conditions generated by the electric or baryon form factor.

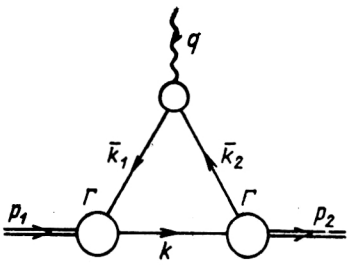

FIG. 6. Electromagnetic form factor of the deuteron in the impulse approximation.

The electromagnetic form factor of the deuteron is described by the previous diagram of Fig. 2, which after transition to the conjugate field for the spectator is represented in the form shown in Fig. 6. The momenta $k_{1,2}$ of the active antinucleons are, of course, $-k_{1,2}$. The spinor ring in the diagram corresponds to taking the trace. After transition to the light-cone variables and integration with respect to k_- in complete analogy with the scalar case, the substitution $(m^2-k^2)^{-1}\to 2\pi\,\mathrm{i}\delta(m^2-k^2)\theta(k_0)\theta(p_+-k_+)$ is made, and instead of (14) we obtain

$$F^\mu_{\alpha\beta}(q)=\int (d^4k/(2\pi)^4\mathrm{i})2\pi\mathrm{i}\delta(m^2-k^2)\theta(k_0)\theta(p_+-k_+)\times\mathrm{Sp}\{f^\mu(q,k)\bar{\psi}_\alpha(k_1)(m+\hat{k})\psi_\beta(k_2)\}. \tag{41}$$

Here, f_μ is the form factor of the active nucleon with unity subtracted on account of the trace that derives on the transition in the form factor f^μ from the antinucleon to the nucleon. If desired, a transition can be made in the integral (41) to the variables x and $k_\perp$. Then $k^2_{1,2}$ will be expressed by the previous formulas (18).

In accordance with the impulse approximation, we take the nucleon form factor f^μ on the mass shell of the nucleon. Then it is parametrized by two scalar functions:

$$f^\mu=\gamma^\mu f_1(q^2)+(\mathrm{i}\sigma^{\mu\nu}q_\nu/2m)f_2(q^2), \tag{42}$$

which characterize the electric and magnetic structure of the nucleon. We recall that the electric, f_e, and magnetic, f_M, form factors are related to f_i, $i=1,2$, by

$$f_e=f_1+f_2q^2/4m^2,\quad f_M=f_1+f_2. \tag{43}$$

The deuteron form factor $F^\mu_{\alpha\beta}$ contains three scalar components of $p=\frac{1}{2}(p_1+p_2)$:

$$F^\mu_{\alpha\beta}=-2p^\mu g_{\alpha\beta}F_1(q^2)+(q_\alpha g^\mu_\beta-q_\beta g^\mu_\alpha)F_2(q^2)+(2p^\mu q_\alpha q_\beta/M^2)F_3(q^2), \tag{44}$$

which are related to the electric, F_e, magnetic, F_M, and quadrupole, F_Q, form factors by

$$F_e=F_1+\tfrac{2}{3}\eta F_Q, \quad F_M=F_2,$$
$$F_Q=F_1-F_2+(1+\eta)F_3, \tag{45}$$

where $\eta = -q^2/4M^2$.

Substituting the expressions (42) and (40) for f_μ and ψ_α in the integrand in (41), calculating the traces, and analyzing the structure of the integral with respect to the indices α, β, and μ, we can express the deuteron form factors and F_i in terms of integrals with respect to x and $k_\perp$ of linear combinations $u_i(k_1^2)u_j(k_2^2)$, $i, j = 1,...,4$. The corresponding expressions are very cumbersome and are given in Ref. 26.

The final expressions for the form factors F_i can be expressed in the form

$$F_i=f_1A_i+f_2B_i, \quad i=1,...,3, \tag{46}$$

in which we have separated the dependence of F_i on the nucleon form factors f_1 and f_2. The functions A_i and B_i describe the intrinsic structure of the deuteron.

5. CONSTRUCTION OF A RELATIVISTIC DEUTERON WAVE FUNCTION

As we said, we intend to determine the deuteron wave function semiphenomenologically, in the first place by requiring correspondence with the nonrelativistic deuteron wave functions. As in the scalar case, the equation for the wave function with allowance for spins goes over in the deuteron rest frame in the nonrelativistic limit into a Schrödinger equation. Then from the relativistic propagator $(m + \hat{k}_1)^{-1}$ in $\psi_\alpha(k_1)$ there survives only the positive-frequency contribution $u^c(k_1)\hat{u}^c(k_1)/(\sqrt{m^2+\mathbf{k}_1^2} - k_{10})2\sqrt{m^2+\mathbf{k}_1^2}$. In the nonrelativistic limit, $\sqrt{m^2+\mathbf{k}_1^2} - k_{10} \simeq (\mathbf{k}^2/m + \varepsilon)$, where ε is the deuteron binding energy. One of the two spinors u^c and $\bar{u}_c$ occurs in the definition of the nonrelativistic limit of the potential. Thus, apart from the normalization the wave function is determined in the nonrelativistic limit by the expression

$$\Phi_\mu(\mathbf{k})=(\mathbf{k}^2+\alpha^2)^{-1}\bar{u}_p(\mathbf{k})\Gamma_\mu\bar{u}_n^c(\mathbf{k}_1), \quad k_1^2\to m^2, \ \alpha^2=m\varepsilon, \tag{47}$$

where Γ_μ is the *dpn* vertex, related to ψ_μ by $\psi_\mu = \Gamma_\mu(m + \hat{k}_1)^{-1}$. If Γ_α is represented in a form analogous to (40),

$$\Gamma_\alpha=k_\alpha[a_1+a_2(m+\hat{k}_1)]+\gamma_\alpha[a_3+a_4(m+\hat{k}_1)], \tag{48}$$

where $a_i = a_i(k_1^2)$ are four functions related simply to u_i, then in the nonrelativistic limit we find from (47) the following expressions for the spatial components Φ_μ, $\mu = 1, 2, 3$:

$$\Phi_i(\mathbf{k})=\frac{\sqrt{m}}{2}(\mathbf{k}^2+\alpha^2)^{-1}\chi_p^* \times\left\{\tilde{c}\sigma_i+\frac{\mathbf{k}^2}{m}\left(\tilde{a}-\frac{\tilde{c}}{2m}\right)\boldsymbol{\sigma}\,\mathbf{n}n_i\right\}\chi_n^c. \tag{49}$$

Here, $\mathbf{n} = \mathbf{k}/k$, and χ and σ are spinors and Pauli matrices, respectively. The functions with $\tilde{c}(k_1^2)$ and $\tilde{a}(k_1^2)$ are linear combinations of $a_i(k_1^2)$:

$$\tilde{c}=a_3-a_4(m^2+k_1^2)/2m, \quad \tilde{a}=a_1+a_2(m^2-k_1^2)/2m, \tag{50}$$

and the dependence on $\mathbf{k}^2$ is determined from (38). It can be seen that the nonrelativistic limit is sensitive to only two of the four wave functions of the relativistic deuteron.

It is well known that the wave function of the nonrelativistic deuteron can be expressed in terms of the standard S and D components $u(\mathbf{k}^2)$ and $\omega(\mathbf{k}^2)$ by

$$\Phi_i(\mathbf{k}^2)=\sqrt{2\pi}\chi_p^*\left\{u\sigma_i-\frac{1}{\sqrt{2}}w(3n_i(\boldsymbol{\sigma}\mathbf{n})-\sigma_i)\right\}\chi_n^c, \tag{51}$$

where the normalization has the form

$$\int k^2dk(u^2+w^2)=1. \tag{52}$$

Comparison of (49) and (51) makes it possible to relate the components of the relativistic wave function a_i (and, with them, u_i also) in the nonrelativistic limit to the well-known S and D waves u and w. The precise connection requires allowance for the normalization condition. Taking it as the asymptotic normalization, i.e., the behavior of the wave function at large distances, or, equivalently, the *dpn* coupling constant when all three particles are physical, we find the relations

$$\left.\begin{aligned}&\tilde{c}=\sqrt{8\pi/m}(\alpha^2+\mathbf{k}^2)[u+w/\sqrt{2}];\\&\tilde{a}=\sqrt{8\pi/m}(\alpha^2+\mathbf{k}^2)[-3mw/\mathbf{k}^2\sqrt{2}+(u+w/\sqrt{2})/2m];\\&k_1^2\to m^2.\end{aligned}\right\} \tag{53}$$

We shall construct relativistic wave functions $a_i(k_1^2)$ as sums of pole terms, choosing the positions of the poles in accordance with the analytic properties:

$$\left.\begin{aligned}a_{1,3}(k_1^2)/(m^2-k_1^2)&=\sum_1^N \xi_i^{(1,3)}/(t_i-k_1^2);\\a_{2,4}(k_1^2)/(m^2-k_1^2)&=\sum_2^L \xi_i^{(2,4)}/(t_i-k_1^2),\end{aligned}\right\} \tag{54}$$

where $t_1 = m^2$, $t_i > m^2$ for $i > 1$. Such a representation is convenient because the well-known nonrelativistic wave functions u and w are also usually represented in the form of an analogous sum of pole terms with respect to the variable $\mathbf{k}^2$. Therefore, we achieve agreement with the nonrelativistic limit if we choose the poles and residues of these linear combinations $\tilde{a}$ and $\tilde{c}$ in accordance with the known poles and residues of the nonrelativistic wave functions in order to achieve fulfillment of (53) in the nonrelativistic limit. At the same time, some of the residues ξ_i remain free, since there are four, and not two, relativistic wave functions. Let $N \geqslant L$ and N be chosen in accordance with the number of poles of the nonrelativistic wave function. The conditions of convergence of the integrals with respect to $k_+, k_\perp$ for the form factors impose certain restrictions on the behavior of a_i when $|k_1^2| \to \infty$; they require a decrease of $a_{1,3}$ and $k_1^2 a_{2,4}$. This gives six further conditions on the residues, three of which are satisfied in the nonrelativistic limit, while three are new. The upshot is that there remain $2(L-1)-3 = 2L-5$ unknown residues. They can be

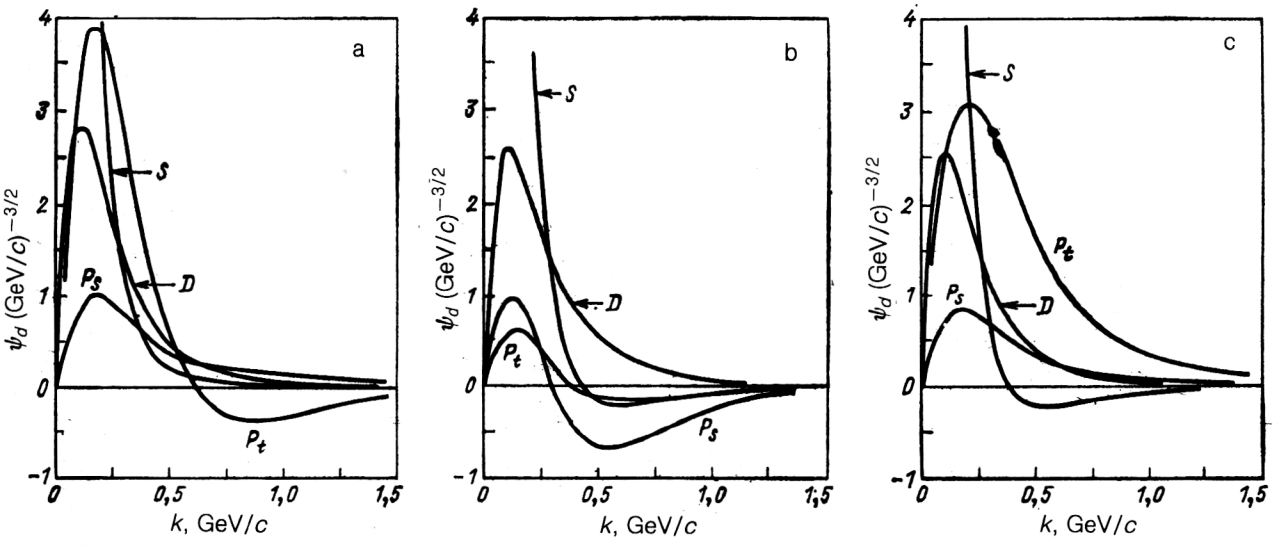

FIG. 7. Relativistic deuteron wave functions of the S, P, and D waves without core (a, Ref. 26), with core (b, Ref. 27), and of Gross (c, Ref. 19).

determined, for example, from the normalization of the electromagnetic form factors of the deuteron at the origin, i.e., from the known charge, magnetic, and quadrupole moments of the deuteron:

$$F_e(0)=1, \quad F_M(0)=\mu_d, \quad F_Q(0)=Q_d. \tag{55}$$

In Refs. 26 and 27, numerical calculations were made for two nonrelativistic deuteron wave functions with parameters taken from Refs. 33 and 34. The first of these contained four, and the second—currently the best—13 pole terms in each of the S and D waves. In both cases, the number of terms in the representation of the functions $a_{2,4}$ is 3. The results of the optimal choice of the free parameters $\xi_4^{(2)}$ and $\xi_{3,4}^{(4)}$ together with the remaining parameters of the relativistic wave function are presented in Refs. 26 and 27. In Ref. 25, the wave function from Ref. 35 was used as the nonrelativistic wave function. It contains six pole terms in the S wave and five in the D wave. The parametrization of this relativistic wave function is given in Ref. 25.

The amplitude for transition of the deuteron into two nucleons, one virtual and the other on the mass shell, can be expressed in terms of the vertex function Γ_α and represented as a sum of relativistic deuteron wave functions with positive, ψ^+, and negative, ψ^-, energies:[19]

$$\psi^+(\mathbf{k})=A\bar{u}(\mathbf{k})\Gamma_\alpha(\mathbf{k})C\bar{u}^T(-\mathbf{k})\xi^\alpha; \tag{56}$$

$$\psi^-(\mathbf{k})=B\bar{u}(\mathbf{k})\Gamma_\alpha(\mathbf{k})C\bar{v}^T(-\mathbf{k})\xi^\alpha. \tag{57}$$

Here $A=[8\sqrt{\pi^3 M}E(2E-M)]^{-1}$; $B=-[8\sqrt{\pi^3 M}EM]^{-1}$; $E=\sqrt{m^2+\mathbf{k}^2}$; u and v are Dirac spinors; C is the matrix of charge conjugation; and ξ is the polarization vector. In the deuteron rest frame, these functions are related to the wave functions of the S, P, and D waves, denoted by u, $v_{s,t}$, and w, respectively, as follows:

$$\psi^+(\mathbf{k})=(4\pi)^{-1/2}\chi_p^*\{u(\sigma\xi)+w \times[(\sigma\mathbf{n})(\xi\mathbf{n})-(\sigma\xi)]/\sqrt{2}\}\chi_n^c; \tag{58}$$

$$\psi^-(\mathbf{k})=(3/4\pi)^{1/2}\chi_p^*\{v_s(\mathbf{n}\xi)+v_t \times[(\sigma\mathbf{n})(\sigma\xi)-(\mathbf{n}\xi)]/\sqrt{2}\}\chi_n^c. \tag{59}$$

Comparing the expressions (56), (57), (58), and (59), we find relations that connect the two sets of functions $a_i(k)$ $(i=1,...,4)$ and u, $v_{s,t}$, w:

$$u=N_s[a_1\mathbf{k}^2+a_3(2E+m)+a_4(2E-M) \times(E-2m)]; \tag{60}$$

$$v_s=N_p|\mathbf{k}|(a_1 m-a_3+a_2 ME); \tag{61}$$

$$v_t=N_p|\mathbf{k}|\sqrt{2}a_4 M; \tag{62}$$

$$w=N_D[a_1\mathbf{k}^2+a_3(m-E)+a_4(E-m)(2E-M)], \tag{63}$$

where $N_s=N_D/\sqrt{2}=[3\pi\sqrt{2M}(2E-M)]^{-1}$; $N_p=-[\pi\sqrt{6ME}M]^{-1}$.

Figure 7a shows graphs of the relativistic deuteron wave functions u, $v_{e,t}$, w obtained by relativizing the wave functions of Ref. 33. A feature of these is the absence of a core in the S wave, this being reflected in the monotonic decrease of the graph of the function $u(k)$. The graphs of the dependence of w and $v_{s,t}$ (D and P waves) begin at the origin and then increase monotonically, reaching a maximum. At large $|\mathbf{k}|$, v_s and w decrease monotonically, approaching zero from positive values, while v_t, having reached a minimum, increases monotonically, approaching zero from negative values.

Figure 7b shows graphs of the relativistic deuteron wave function of Ref. 27 obtained by relativizing the "Paris" wave function.[34] This takes into account the presence of a core in the S wave, manifested in the characteristic behavior of the graph of u in the region $0.4<k<0.5$ GeV/c and known in the literature as dynamic enhance-

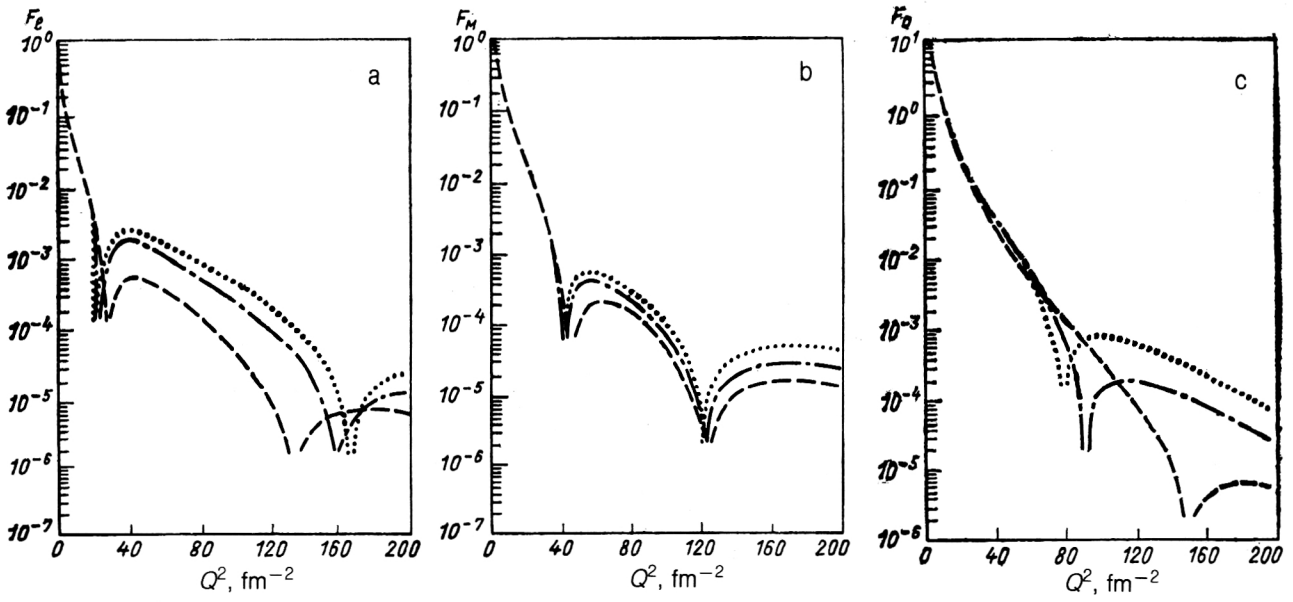

FIG. 8. Electric, $F_e(Q^2)$ (a), magnetic, $F_M(Q^2)$ (b), and quadrupole, $F_Q(Q^2)$ (c), form factors of the deuteron in the impulse approximation.

ment of the D wave. In this region there must be the strongest manifestation of effects due to the quark–gluon structure of nucleons such as quark filling of the core[36] and elongation of the nucleon.[37] The behavior of w is analogous to the case in Fig. 7a. The graphs of $v_{s,t}$ have oscillatory behavior at $k<0.6$ GeV/c. Outside this region, a monotonic decrease is observed. Note that the behavior of $v_{s,t}$ for a relativistic wave function with a core is very different from the behavior for a wave function without a core (Fig. 7a). In our opinion, this is due to the difference in the behavior of the nonrelativistic deuteron wave function in the region of the core.

For comparison, Fig. 7c gives graphs of the relativistic wave equations obtained by solving Gross's equation.[19] It can be seen from Fig. 7c that the behavior of the S and D components of the relativistic wave function is analogous to the behavior of these functions in Fig. 7b. The graph of v_s agrees well with the analogous graph in Fig. 7a but differs appreciably from the graph of v_s in Fig. 7b. The behavior of v_t is different for all three cases.

It can be seen from Figs. 7b and 7c that for the relativistic wave function with core the main difference is observed in the behavior of the antinucleon components $v_{s,t}$.

In the covariant approach in light-cone variables of Refs. 25–27, allowance is made for not only the spectator pole but also the contribution from the pole of the active nucleon. At the same time, the kinematic suppression of the contribution of the antinucleon components compared with the nucleon contribution is automatically taken into account. This is the fundamental difference from Gross's approach. In that approach, the deuteron is treated in the rest frame, where there is no such restriction. At the same time, absence of information about the physically observable component of the relativistic deuteron wave function introduces an uncertainty into the solution of Gross's equation in the behavior of the physically observable nucleon component in the relativistic region. All this indicates that the choice of the frame of reference has fundamental importance in the realization of a definite procedure for constructing a relativistic deuteron wave function.

In conclusion, we note that the structure of the S and D components of the constructed deuteron wave functions is qualitatively similar to the structure of the corresponding nonrelativistic components. However a slower decrease with increasing k is observed for the components of the relativistic wave function. When the relativization procedure is carried out, the behavior of the P wave functions does not exhibit clearly expressed effects, and unambiguous conclusions about its structure cannot be drawn.

6. CALCULATIONS OF ELECTROMAGNETIC FORM FACTORS OF THE DEUTERON FOR ELASTIC *ed* SCATTERING

Having at our disposal the deuteron wave function ψ_α defined as the sum of pole terms (54) with the positions of the poles and residues determined in accordance with the scheme described in the previous section, we can proceed to calculations of experimentally observable quantities associated with interaction of the deuteron with particles and fields. In this section, we give the results of calculations of the electromagnetic form factors of the deuteron in accordance with the expressions obtained in Sec. 4, and also the intimately related calculations of the cross section for elastic *ed* scattering.

In Fig. 8, we give the results of calculation of the electric, F_e, magnetic, F_M, and quadrupole, F_Q, form factors of the deuteron. In the calculations for the proton form factors we used the dipole formula

$$f_M^p(Q^2)=\mu_p(1+Q^2/0.71)^{-2} \tag{64}$$

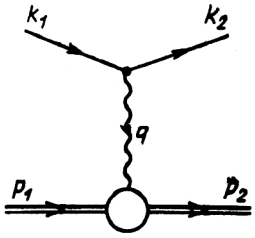

FIG. 9. Amplitude of elastic *ed* scattering in the single-photon approximation.

and the scaling law

$$f_e^p(Q^2)=f_M^p(Q^2)/\mu_p. \tag{65}$$

The magnetic form factor of the neutron is reasonably well described by the dipole formula

$$f_M^n(Q^2)=\mu_n(1+Q^2/0.71)^{-2}, \tag{66}$$

and for the electric form factor we chose the parametrization

$$f_e^n(Q^2)=-\frac{\tau}{1+p\tau}f_M^n(Q^2), \tag{67}$$

where $\tau = Q^2/4m^2$, and p is a numerical parameter that is poorly determined from the experiments. A justification of the choice of the parameter p for the potentials can be found in Refs. 38 and 39. Other parametrizations of the nucleon form factors are described in Refs. 40 and 41.

In Fig. 8, the broken, chain, and dotted curves correspond to choices of the parameter p equal to 0, 1, and ∞, respectively. It can be seen that with increasing p there is a displacement of the first zero of all form factors to larger Q^2. This dependence is manifested especially clearly for $F_Q(Q^2)$.

The results indicate a strong dependence on the choice of the electric form factor of the neutron. Great interest therefore attaches to polarization experiments, in which it is in principle possible to obtain independent information about each of the deuteron form factors. Such experiments could also give additional information about the electric form factor of the neutron at large Q^2.

Knowledge of the form factors makes it possible to describe completely the process of elastic *ed* scattering in the single-photon approximation (Fig. 9). Its amplitude is determined by the expression

$$M=\bar{u}(k_2,\sigma_2)\gamma_\mu u(k_1,\sigma_1)e^*_{2\alpha}(p_2,\zeta_2)\Gamma_\mu^{\alpha\beta}e_{1\beta}(p_1,\zeta_1)e^2/(-q^2). \tag{68}$$

Here $k_{1,2}(p_{1,2})$ are the momenta of the electron (respectively, deuteron) in the initial and final states; q is the proton momentum; $e_{1,2}$ are the deuteron polarization vectors; and $\Gamma_\mu^{\alpha\beta}$ is the electromagnetic form factor. It can be seen that the amplitude is completely determined if the form factor $\Gamma_\mu^{\alpha\beta}$ is known.

The differential cross section for scattering of unpolarized particles has the form

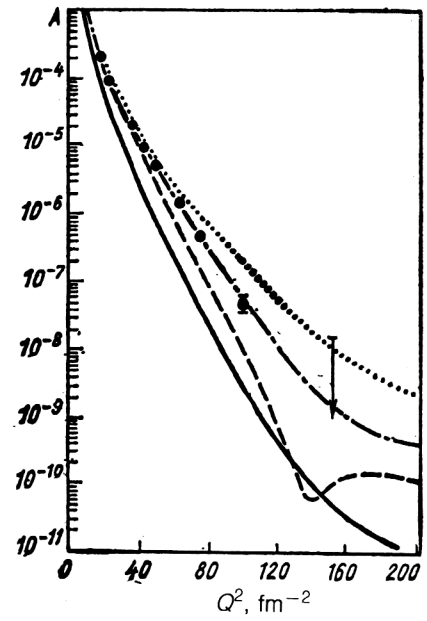

FIG. 10. Structure function $A(Q^2)$ in the impulse approximation.

$$d\sigma/d\Omega=(d\sigma/d\Omega)_0[A(Q^2)+B(Q^2)\mathrm{tg}^2\theta/2], \tag{69}$$

where $(d\sigma/d\Omega)_0 = [\alpha^2\cos^2(\theta/2)/4E^2\sin^4(\theta/2)][1+2(E/m_e)\sin^2(\theta/2)]^{-1}$ is the cross section for scattering by a point particle; θ and E are the scattering angle and the initial energy of the electron in the laboratory system; and $\alpha = e^2/4\pi$. The structure functions $A(Q^2)$ and $B(Q^2)$ are expressed in terms of the electromagnetic form factors of the deuteron by the well-known formulas[42–44]

$$A(Q^2)=F_e^2(Q^2)+\tfrac{2}{3}\eta F_M^2(Q^2)+\tfrac{8}{9}\eta^2F_Q^2(Q^2); \tag{70}$$

$$B(Q^2)=\tfrac{4}{3}\eta(1+\eta)F_M^2(Q^2), \quad \eta=Q^2/4M^2. \tag{71}$$

In Figs. 10 and 11 we give graphs of the calculated structure functions $A(Q^2)$ and $B(Q^2)$ from Refs. 26 and 27. The dependence of $A(Q^2)$ and $B(Q^2)$ on the choice of the electric form factor of the neutron (67) was investigated. In all the figures, the graphs of $A(Q^2)$ and $B(Q^2)$ for the three values 0, 1, and ∞ of the parameter p are shown by the broken, chain, and dotted curves, respectively.

In Fig. 10, the continuous curve shows Gross's calculation,[20] which does not use light-cone variables but does use the same expressions for the nucleon form factors with $f_e^n(Q^2) = 0$. The results that we obtained for $A(Q^2)$ indicate a strong dependence on the choice of the electric form factor of the neutron in the region $Q^2 > 30$ fm^{-2}. Good agreement with the experimental data[45,46] is obtained for $p = 1$. Gross's calculation[20] lies appreciably below our calculation ($p = \infty$) and below the experimental data. Note that the graph of $A(Q^2)$ for the case $p = \infty$ differs qualitatively from the other two with $p = 0$ and 1. This difference is due to the proximity of the zeros in the electric and quadrupole form factors of the deuteron.

The behavior of the structure function $B(Q^2)$ in Fig. 11a does not exhibit in the considered region a significant

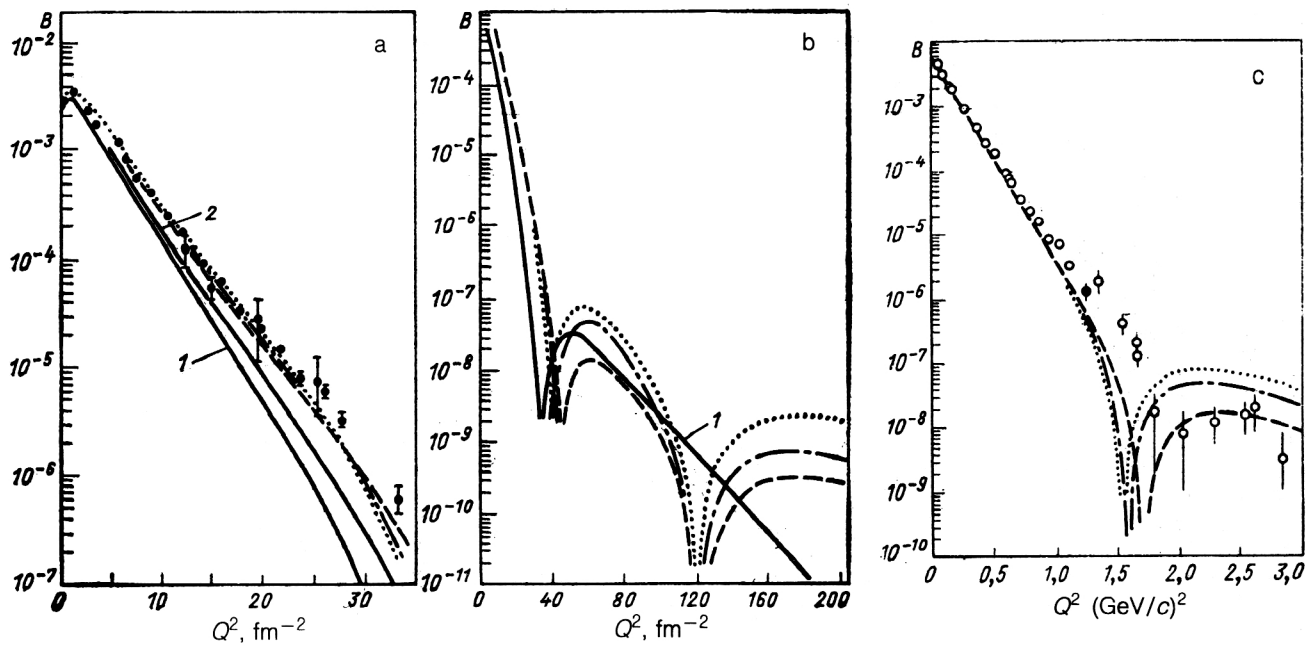

FIG. 11. Structure function $B(Q^2)$ in the impulse approximation. The broken, chain, and dotted curves are the results of calculations with p equal to 0, 1, ∞, respectively: (a) 1) Gross's calculation in Ref. 20; 2) the calculations of Ref. 48, experimental data from Ref. 47; (b) 1) the calculation of Gross in Ref. 20; (c) experimental data from Refs. 49 and 50.

dependence on the parameter p. For $Q^2 < 25$ fm^{-2}, we observe good agreement with the experimental data of Ref. 47. In the region $Q^2 > 25$ fm^{-2}, our calculation lies somewhat below the experimental points.

For comparison, in Fig. 11a we give the results of calculation in the impulse approximation from Refs. 20 and 48. The first calculation (curve 1) used relativistic wave functions that are solutions of Gross's equation[19] and expressions for the deuteron form factors obtained in the deuteron rest frame. The second calculation (curve 2)[48] used relativistic deuteron wave functions obtained by solving the Bethe–Salpeter equation, while the calculation of the form factors was made, as in Gross's approach, in the deuteron rest frame but using different expressions. As can be seen from Fig. 11a, the graphs of these functions lie below our curve and do not describe the experimental data.

Figure 11b gives the graph of $B(Q^2)$ in a wider range of momentum transfers than in Fig. 11a. It can be seen that with increasing p there is a displacement of the zeros of $B(Q^2)$ to larger Q^2. At the same time, the values of the second and third maxima are decreased by about an order of magnitude. The continuous curve gives Gross's calculation.[20] It can be seen that compared with our calculation (p equal to 0, 1, ∞) appreciable qualitative and quantitative differences are observed.

In Fig. 11c, our calculation of $B(Q^2)$ is compared with the most recent experimental data.[49,50] It can be seen from Fig. 11c that for $Q^2 < 0.7$ (GeV/c)^2 the theoretical curves give a good description of the experimental data. In the region $Q^2 > 0.7$ (GeV/c)^2 a systematic lowering of the calculated curves is observed, and the first zero is shifted to smaller Q^2 than in the experiments. At the same time, it should be noted that there is good qualitative agreement with experiment for all three curves.

It can be seen from (70) and (71) that for scattering of unpolarized particles it is impossible to separate the contributions from the charge and quadrupole form factors but that this can be done in experiments with polarized particles.

Thus, in the case of scattering of longitudinally polarized electrons by an unpolarized deuteron target, the recoil deuterons acquire vector and tensor polarizations. They can be expressed in terms of the electromagnetic form factors of the deuteron by the well-known formulas[21]

$$p_x I_0 = -\frac{4}{3}[\eta(1+\eta)]^{1/2} F_M \left(F_e + \frac{1}{3}\eta F_Q\right) \operatorname{tg}\frac{\theta}{2}; \tag{72}$$

$$p_z I_0 = \frac{2}{3}\eta \left\{(1+\eta)\left[1+\eta \sin^2\frac{\theta}{2}\right]\right\}^{1/2} F_M^2 \operatorname{tg}\frac{\theta}{2}\sec\frac{\theta}{2}; \tag{73}$$

$$p_{zz} I_0 = -\frac{8}{3}\eta F_e F_Q - \frac{8}{9}\eta^2 F_Q^2 - \frac{1}{3}\eta \times \left[1 + 2(1+\eta)\operatorname{tg}^2\frac{\theta}{2}\right] F_M^2; \tag{74}$$

$$(p_{xx} - p_{yy}) I_0 = -\eta F_M^2; \tag{75}$$

$$p_{xz} I_0 = -2\eta \left[\eta + \eta^2 \sin^2\frac{\theta}{2}\right]^{1/2} F_M F_Q \sec\frac{\theta}{2}; \tag{76}$$

$$T_{20} = p_{zz}/\sqrt{2}, \tag{77}$$

where $I_0 = A(Q^2) + B(Q^2)\operatorname{tg}^2(\theta/2)$.

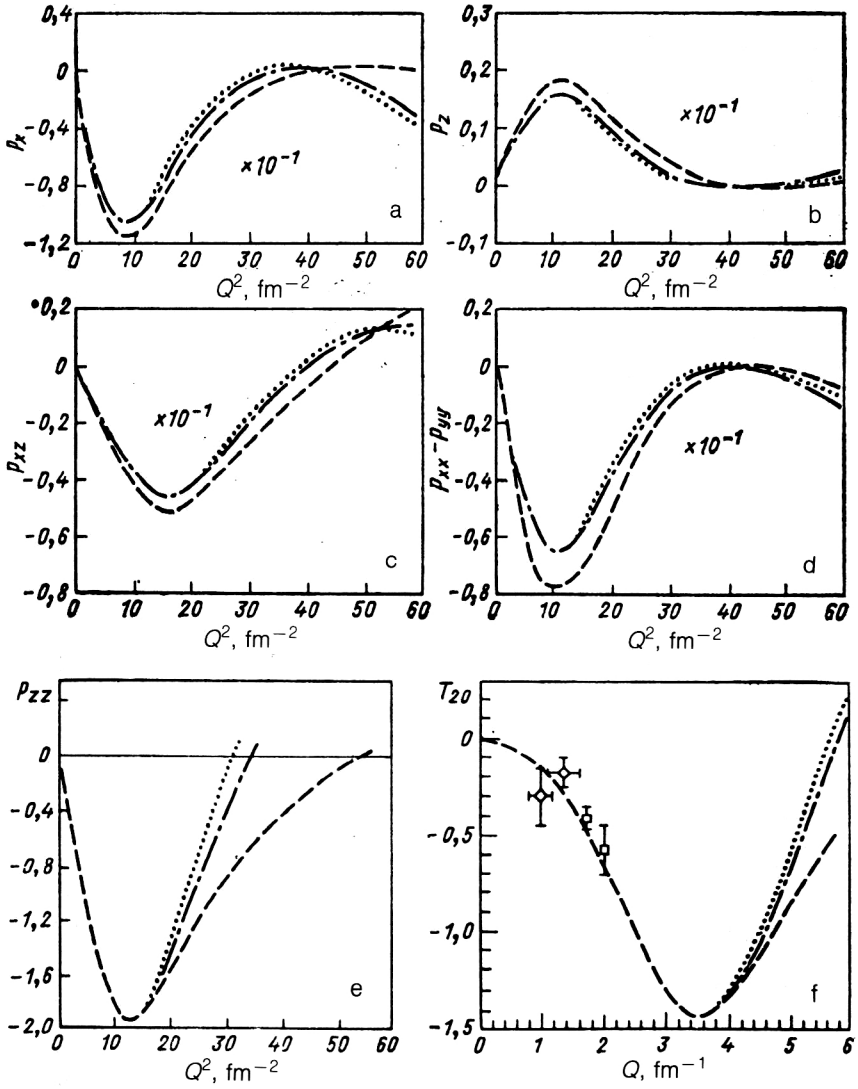

FIG. 12. Vector p_x (a), p_z (b), and tensor, P_{xz} (c), $p_{xx} - p_{yy}$ (d), p_{zz} (e), T_{20} (f) polarizations of the deuteron in elastic *ed* scattering in the impulse approximation at $\theta_{e'} = 40°$.

Figure 12 shows calculations of the vector, p_x, p_z, and tensor, p_{xz}, $p_{xx} - p_{yy}$, p_{zz}, T_{20} polarization characteristics of the scattering of longitudinally polarized electrons by an unpolarized deuterium target with detection of the polarized recoil deuterons and the scattered electron at angle $\theta_e = 40°$. It can be seen from Fig. 12 that as the parameter p is increased, the point of intersection of the graphs with the Q^2 axis is displaced to larger Q^2. A significant difference between our calculation and the analogous calculation of Gross[21] is observed in the region $Q^2 > 10$ fm^{-2}. In our calculations, the points of intersection of the graphs lie in the interval $30 < Q^2 < 50$ fm^{-2}, but in the calculations of Ref. 21 they lie in the interval $15 < Q^2 < 25$ fm^{-2}.

In Fig. 12f, our curve for T_{20} is compared with experiment.[51,52] In the considered region, all three graphs (p equal to 0, 1, ∞) practically coincide and describe the experimental data.

Among these quantities, the greatest interest attaches to measurement of p_{zz} and p_x/p_{xz} (Fig. 13), since they include a combination of the charge and quadrupole form factors different from the combination in $A(Q^2)$.

We also consider the elastic scattering of longitudinally polarized electrons by vector-polarized deuterons. The cross section of the process can be represented in the form

$$\frac{d\sigma}{d\Omega_e} = \frac{\alpha^2}{q^4}\frac{\varepsilon_2}{\varepsilon_1}\frac{l_{\mu\nu}W^{\mu\nu}_{\alpha\beta}\rho^{\alpha\beta}}{1+2\dfrac{\varepsilon_1}{M}\sin^2\dfrac{\theta}{2}}, \tag{78}$$

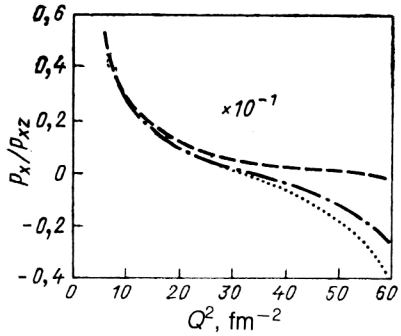

FIG. 13. Dependence of the ratio p_x/p_{xz} on the momentum transfer Q^2 in elastic *ed* scattering in the impulse approximation at $\theta_{e'} = 40°$.

where $\varepsilon_{1(2)}$ is the energy of the electron in the initial (respectively, final) state, and θ is the emission angle of the scattered electron. The tensor $l_{\mu\nu}$ describes the amplitude of the process of scattering of a virtual photon by a polarized electron, $\gamma^* + \vec{e} \to \gamma^* + \vec{e}$, and is determined by the well-known expression

$$l_{\mu\nu}=2(k_{1\mu}k_{2\nu}+k_{1\nu}k_{2\mu})+g_{\mu\nu}g^2+2im_e\varepsilon_{\mu\nu\sigma\lambda}s_e^\sigma q^\lambda. \tag{79}$$

The polarization density matrix of the deuteron has the form

$$\rho_{\alpha\beta}=-(g_{\alpha\beta}-p_{1\alpha}p_{1\beta}/M^2)/3+i\varepsilon_{\alpha\beta\sigma\lambda}p_1^\sigma s_d^\lambda/2M. \tag{80}$$

The tensor $W_{\mu\nu}^{\alpha\beta}$ describes the amplitude for scattering of the virtual photon by the vector-polarized deuteron, $\gamma^* + \vec{d} \to \gamma^* + \vec{d}$, and is expressed by

$$W_{\mu\nu}^{\alpha\beta}=\Gamma_\nu^{\alpha\sigma}(p_1,p_2,q)\rho_{\sigma\lambda}(p_2)\Gamma_\mu^{\lambda\beta}(p_1,p_2,q). \tag{81}$$

Here, $\Gamma_\nu^{\alpha\sigma}$ is the electromagnetic deuteron vertex. The contraction $W_{\mu\nu}=\rho_{\alpha\beta}W_{\mu\nu}^{\alpha\beta}$ is usually parametrized as follows:

$$\begin{aligned}W_{\mu\nu}=&-(g_{\mu\nu}-q_\mu q_\nu/q^2)W_1^d+p_\mu p_\nu W_2^d/4M^2\\&+i\varepsilon_{\mu\nu\sigma\lambda}q^\sigma\{s_d^\lambda MG_1^d+[p_1^\lambda(qs_d)\\&-s_d^\lambda(qp_1)]M^{-1}G_2^d\}.\end{aligned} \tag{82}$$

The structure functions $W_{1,2}^d$ and $G_{1,2}^d$ can be expressed in terms of the electromagnetic form factors of the deuteron:

$$W_1^d=2M^2B(Q^2),\quad W_2^d=4M^2A(Q^2); \tag{83}$$

$$G_1^d=2F_M[F_e+F_M\eta/2+F_Q\eta/3]; \tag{84}$$

$$G_2^d=-F_M[F_e-F_M/2+F_Q\eta/3]. \tag{85}$$

The longitudinal, $A_\parallel$, and transverse, $A_\perp$, asymmetries of the process of elastic scattering of the polarized electrons by the vector-polarized deuterons can be defined as follows:

$$A_\parallel=(\sigma'(\uparrow\uparrow)-\sigma'(\uparrow\downarrow))/(\sigma'(\uparrow\uparrow)+\sigma'(\uparrow\downarrow)); \tag{86}$$

$$A_\perp=(\sigma'(\uparrow\rightarrow)-\sigma'(\uparrow\leftarrow))/(\sigma'(\uparrow\rightarrow)+\sigma'(\uparrow\leftarrow)). \tag{87}$$

Here $(\uparrow\uparrow)$ and $(\uparrow\downarrow)$ denote parallel and antiparallel orientation of the polarization vectors $\mathbf{s}_e$ and $\mathbf{s}_d$, and $(\uparrow\rightarrow)$ corresponds to the case in which the vectors $\mathbf{s}_e$ and $\mathbf{s}_d$ are mutually orthogonal; $\sigma' \equiv d\sigma/d\Omega_e$.

The asymmetries $A_\parallel$ and $A_\perp$ can be expressed in terms of the structure functions $W_{1,2}^d$, $G_{1,2}^d$:[41,53]

$$A_\parallel=2\operatorname{tg}^2\frac{\theta}{2}[(\varepsilon_1+\varepsilon_2\cos\theta)MG_1^d-Q^2G_2^d]/\left[W_2^d+2W_1^d\operatorname{tg}^2\frac{\theta}{2}\right]; \tag{88}$$

$$A_\perp=2\operatorname{tg}^2\frac{\theta}{2}(MG_1^d+2\varepsilon_1G_2^d)\varepsilon_2\sin\theta/\left[W_2^d+2W_1^d\operatorname{tg}^2\frac{\theta}{2}\right]. \tag{89}$$

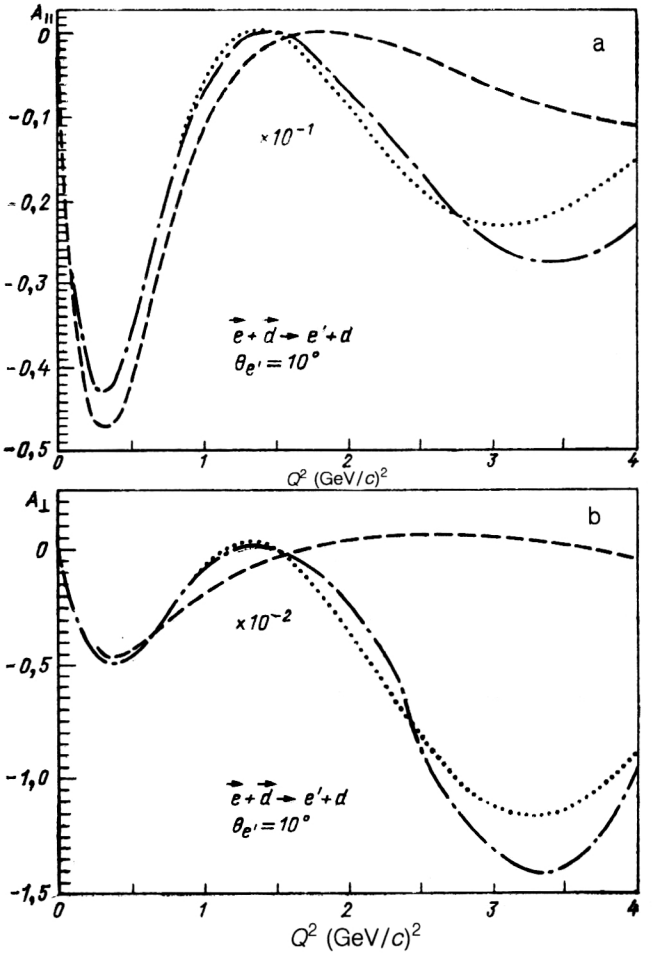

FIG. 14. Longitudinal, $A_\parallel(Q^2)$ (a), and transverse, $A_\perp(Q^2)$ (b), asymmetries of the $\vec{ed} \to e'd$ process in the single-photon approximation. The broken, chain, and dotted curves represent calculations with the wave function of Ref. 27 and with p equal to 0, 1, and ∞, respectively.

Figure 14 gives the results of calculation of the reaction asymmetries $A_\parallel$ and $A_\perp$ as functions of the square D^2 of the momentum transfer for $\theta_e = 10°$. It can be seen from the figure that for $Q^2 < 1.6\ (\text{GeV}/c)^2$ all the curves (p equal to 0, 1, ∞) have qualitatively similar behavior, while for $Q^2 > 1.6\ (\text{GeV}/c)^2$ they differ significantly.

Figure 15 shows the results of calculation of the structure function $G_1^d(Q^2)$ in the impulse approximation. It can be seen from the figure that in the region $Q^2 > 2.0$ GeV/c^2 the curve with $p = \infty$ lies below the curves with p equal to 0 and 1, and the zero of $G_1^d(Q^2)$ is shifted to larger Q^2.

Experimental investigations of the asymmetry of the process $\vec{ed} \to ed$ and the structure functions $G_{1,2}^d(Q^2)$ can give new information about the electromagnetic form factors of the deuteron and the electric form factor of the neutron, and they are also of interest for testing the relativistic theory of the deuteron.

7. DEEP INELASTIC *ed* SCATTERING

As is well known, the inclusive cross section for deep inelastic *ed* scattering can be expressed in terms of the

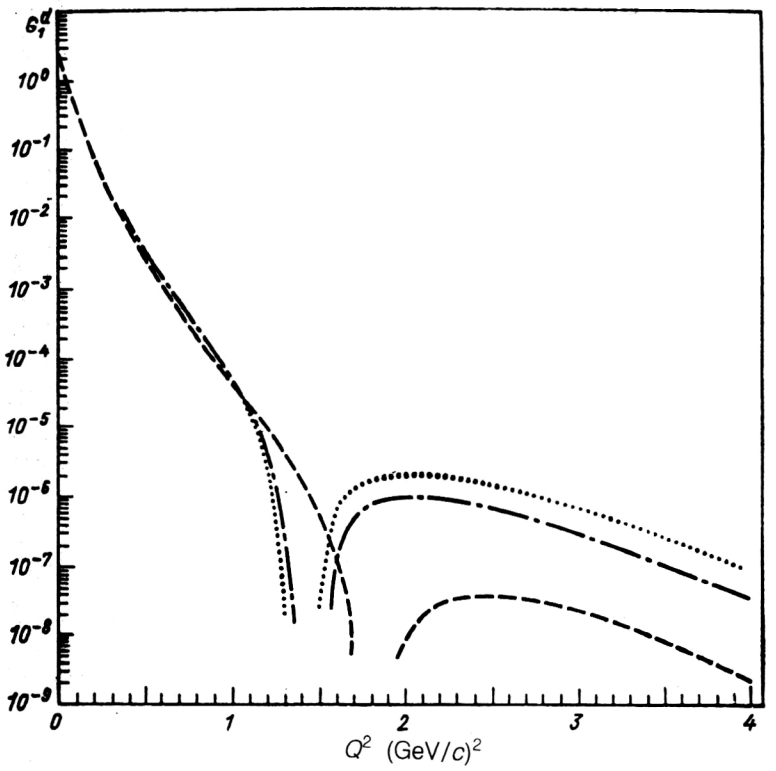

FIG. 15. Structure function $G_1^d(Q^2)$ in the impulse approximation. The broken, chain, and dotted curves represent calculations with the wave functions of Ref. 27 and with p equal to 0, 1, and ∞, respectively.

amplitude for forward scattering of a virtual photon γ^* with momentum q ($q^2 < 0$) by the deuteron. This corresponds to the diagram of Fig. 3 with renotation $l \to q$. When spins are taken into account, the relativistic deuteron wave functions ψ_α appear in the integrand in the expression (25), as in the case of the form factor, and the amplitude a of scattering by the active nucleon becomes a matrix with respect to the spinor indices of the nucleon and the vector indices of the photon ($\mu\nu$). Therefore, we find the amplitude

$$A_{\alpha\beta}^{\mu\nu} = \int [d^4k/(2\pi)^4 i] 2\pi i \delta(k^2 - m^2)\theta(k_0)\theta(p_+ - k_+)\mathrm{Sp}\{a^{\mu\nu}(q,k_1)\bar{\psi}_\alpha(k_1)(m + \hat{k})\psi_\beta(k_1)\}. \tag{90}$$

As we discussed in Sec. 2, at high energies, when $(qp) \equiv \nu \gg m^2$, the quantity $(qk_1) \equiv \nu_1$ is also large, and from all the structures in the amplitude $a^{\mu\nu}(q,k_1)$ there survives only one:

$$a^{\mu\nu}(q,k_1) \simeq (\hat{q}/\nu_1)(g^{(q)\mu\nu}a_1 + k_1^{(q)\mu}k_1^{(q)\nu}a_2). \tag{91}$$

where $g_{\alpha\beta}^{(q)}$ and $k_{1\alpha}^{(q)}$ are, respectively, the metric tensor and a vector orthogonal to q; a_1 and a_2 are invariant functions. If the dependence on the virtuality k_1^2 is ignored, then the imaginary parts of $a_{1,2}$ give the usual structure functions of an unpolarized nucleon:

$$w_i(x_1,Q^2) = \frac{1}{\pi}\,\mathrm{Im}\, a_i, \tag{92}$$

where $Q^2 = -q^2$, $x_1 = Q^2/2\nu_1$. If (90) is averaged over the deuteron polarizations, and the contraction of (90) is taken with the polarization operator ρ_{ab} for the unpolarized deuteron, then the averaged amplitude $A_{\mu\nu} = \rho_{\alpha\beta}A_{\mu\nu}^{\alpha\beta}$ will have a structure analogous to (91):

$$A_{\mu\nu} = g_{\mu\nu}^{(q)}A_1 + p_\mu^{(q)}p_\nu^{(q)}A_2. \tag{93}$$

The deuteron structure functions are related to A_i by a formula that exactly repeats (92):

$$W_i(x,Q^2) = \frac{1}{\pi}\,\mathrm{Im}\, A_i, \tag{94}$$

where $x = Q^2/2\nu$.

We substitute (91) and (40) in the integrand in (90), take the trace, and, analyzing the structure of the integral with respect to the indices $\mu\nu$ after contraction with $\rho^{\alpha\beta}$, find expressions for the amplitude A_i in terms of the bilinear combinations of functions $u_i(k_1^2)u_j(k_1^2)$ and amplitudes a_i for scattering by the nucleon. Taking the imaginary parts of both sides of the equation, we obtain a relation between the structure functions on the deuteron, W_i, and on the nucleon, w_i. If we go over to the usually employed structure functions $F_1^d = 2MW_1^d$, $F_2^d = (\nu/M^2)W_2^d$ and the standard functions $F_{1,2}^N$ for the nucleon, then the relation between F_i^d and F_i^N becomes

$$F_i^d(\alpha,Q^2) = \int_\alpha^1 dx d^2k_\perp \psi_i(x,k_\perp)F_i^N(\alpha/x,Q^2). \tag{95}$$

Here $\psi_1 = \psi_2/x$, and the function ψ_2 gives the probability that the active nucleon carries the fraction x of the $+$ component of the deuteron momentum and the transverse momentum $k_\perp$. It is normalized by the condition

$$\int_0^1 dx \int d^2k_\perp \psi_2(x,k_\perp) = 1 \tag{96}$$

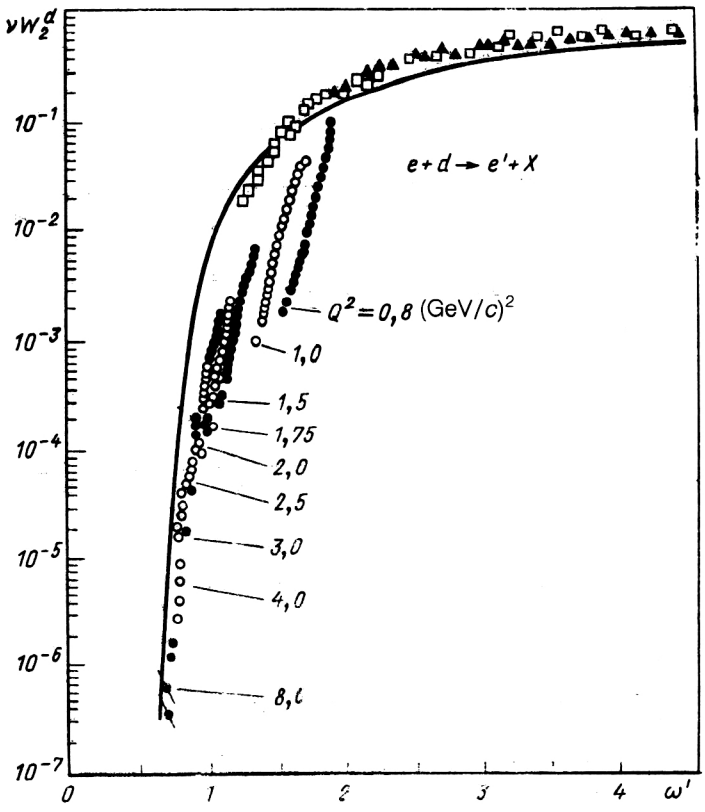

FIG. 16. Structure function νW_2^d of the $ed \to e'X$ process in the impulse approximation. The continuous curve is the result of calculation with the wave function of Ref. 27; the experimental points are from Ref. 55.

and can be expressed in terms of the scalar deuteron wave functions a_i [see the expression (48)] as follows:

$$\begin{aligned}\psi_2(x,k_\perp) = &\{3[a_2k_1^2 - A_3] + 3z[A_2 - 2ma_3A_3 \\ &- a_3^2[M^2 - m^2]] + [k_1^2 - (pk_1)^2/M^2] \\ &\times [A_1^2 - a_1^2k_1^2 - 2A_1a_3 + 2a_1A_3] \\ &+ z[k_1^2 - (pk_1)^2/M^2][-A_1^2 - 2ma_1A_1 \\ &+ 4A_1a_3 + a_1^2(M^2 - m^2) + 4a_1a_3m \\ &- 4a_3^2] + 2[z - (pk_1)/M^2][A_1A_3m \\ &+ (A_1a_3 - a_1A_3)((pk_1) - k_1^2) \\ &- a_1a_3mk_1^2 - A_3^2 + a_3^2k_1^2]\}/ \\ &\times [(m^2 - k_1^2)^2(1-x)3(2\pi)^3], \end{aligned} \tag{97}$$

where $A_1 = a_1m + a_2(m^2 - k_1^2)$, $A_3 = a_3m + a_4(m^2 - k^2)$.

Note that our expression (95) has a similar structure to the expression used, for example, in Refs. 12, 13, and 54. A difference is in the function ψ_2, which in our case does not simply reduce to a sum of squares of the S- and D-wave components of the deuteron wave function but is a combination of all four relativisitic deuteron wave functions.

We now turn to numerical calculations of the deuteron structure functions using the wave functions constructed in Sec. 5.

Figure 16 shows the results of calculation of the structure function νW_2^d at $Q^2 = 6.0$ (GeV/c)^2 as a function of the variable $\omega' = 1/2\alpha + m_N^2/Q^2$, in which one can expect to observe early scaling. For the nucleon structure functions, the standard approximations were chosen:[78]

$$\begin{aligned}F_2^d(x) = &(1-x)^3[1.274 + 0.5989(1-x) \\ &- 1.675(1-x)^2]; \end{aligned} \tag{98}$$

$$F_2^n(x) = (1 - 0.75x)F_2^p(x). \tag{99}$$

Note that to achieve agreement between the calculated curve and the experimental data of Ref. 55 in the cumulative region $0.7 < \omega' < 1.1$ it is necessary to assume a dependence of the parameter m_N^2 on Q^2. In the noncumulative region $\omega' > 2$, the theoretical curve lies somewhat below the experimental points. To test the behavior $\nu W_2^d \sim (1 - x)^9$ at $x \simeq 1$ predicted by the parton model, the cumulative part of the theoretical curve has been approximated by a function of the form $A(\omega' - 0.5)^B$. For the parameters A and B the following values were obtained: $A = 3.96$, $B = 9.25$; $A = 0.12$, $B = 7.25$. In the first calculation, both parameters were selected, and in the second only one (the parameter A was fixed in accordance with Ref. 12, where for B the value 5.7 was obtained).

The results of the calculations show that the theoretical curve basically gives a reasonably good description of the experimental data in both the cumulative ($0.5 < \alpha < 1.0$) and the noncumulative ($0 < \alpha < 0.5$) region.

Figure 17a shows the result of our calculation of the structure function $\nu M_2^d(\alpha, Q^2)$ with the structure function $F_2^N(x,Q^2)$ parametrized in terms of the quark distributions $u(x,Q^2)$, $d(x,Q^2)$, $s(x,Q^2)$ of Ref. 56. It can be seen from

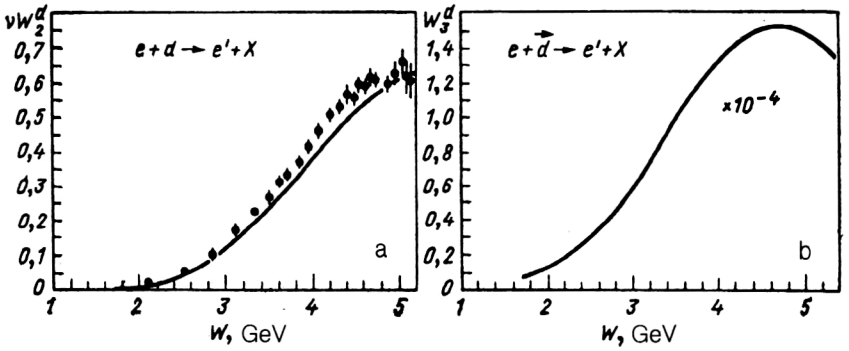

FIG. 17. Structure functions νW_2^d (a) and W_3^d (b) of the $ed \to e'X$ process in the impulse approximation [$\varepsilon_e = 17.0$ GeV; $\theta_{e'} = 18°$; $2 < Q^2 < 14$ $(\text{GeV}/c)^2$]. The continuous curves are the results of calculation with the wave function of Ref. 27; the experimental points are from Ref. 57.

Fig. 17a that our calculation gives a qualitatively good description of the experimental data,[57] and we attribute the difference between the results in the region of large $W = (m^2 - Q^2 + 2q_0 m)^{1/2}$(small α, Q^2) to mass corrections $\sim (m^2/Q^2)^n$.

For electron scattering by tensor-polarized deuterons, a structure $\rho^T_{\alpha\beta} = S_{\alpha\beta}$ appears in the deuteron polarization matrix $\rho_{\alpha\beta}$. Accordingly, in the amplitude of virtual $\gamma^* d$ forward scattering there are additional terms

$$A^{(T)}_{\mu\nu} = \tfrac{1}{2} A_3 \{ p_\mu (S_{\nu\alpha} q^\alpha - q_\nu (qSq)/q^2) + (\mu \rightleftarrows \nu) \}. \quad (100)$$

The imaginary part of A_3 generates the structure function $W_3^d(x, Q^2)$ in accordance with the expression (90).

Figure 17b shows the result of calculation of the structure function W_3^d. For the nucleon structure function $F_2^N(x, Q^2)$, the quark distributions of Ref. 56 were used.

For scattering of polarized electrons by vector-polarized deuterons, the tensor of the structure functions $W_{\mu\nu}$ has the same structure as for the case of elastic ed scattering. Its antisymmetric part is determined by the two structure functions $G^d_{1,2}(\nu, Q^2)$:

$$W^A_{\mu\nu} = i\varepsilon_{\mu\nu\sigma\lambda} q^\sigma \{ s^\lambda M G_1^d + [s^\lambda (pq) - p^\lambda (sq)] M^{-1} G_2^d \}. \quad (101)$$

In the impulse approximation as $\nu, Q^2 \to \infty$ and ignoring G_2^d, we obtain

$$g_1^d(\alpha, Q^2) \varepsilon_{\mu\nu\sigma\lambda} q^\sigma s^\lambda M/\nu = \int_\alpha^1 dx \int d^2 k_\perp \, \mathrm{Sp}\{ \overline{\psi}_\alpha(k_1)(m + \hat{k}_1) \times \psi_\beta(k_1) \hat{q} \sigma_{\mu\nu}/\nu_1 \} \rho^{\alpha\beta} g_1^N(\alpha/x, Q^2). \quad (102)$$

Here $\rho_{\alpha\beta} = i\varepsilon_{\alpha\beta\delta\gamma} s^\sigma p^\lambda / 2M$ is the vector part of the polarization density matrix; g_1^N is the nucleon structure function, $g_1^d = M\nu G_1^d$, and $g_2^d = M^{-1}\nu^2 G_2^d$.

Figure 18 gives the results of the calculation of $\alpha g_1^d(\alpha, Q^2)$ and the asymmetry of the process, defined by

$$A_\parallel(\alpha, Q^2) = \alpha g_1^d(\alpha, Q^2)/F_2^d(\alpha, Q^2). \quad (103)$$

For the nucleon structure functions, the expressions of the Carlitz–Kaur model[58] with quark distributions from Ref. 56 were used.

It can be seen from Fig. 18 that the asymmetry $A_\parallel$ and αg_1^d behave qualitatively in the same way as the corresponding quantities of the process $\vec{\mu}\vec{p} \to \mu X$ in the EMC experiment of Ref. 59. The calculated curve has an asymmetric form. In the region of small α, the curve decreases slowly. In this region, the sea quarks and gluons make an important contribution.

Experimental measurements of $A_\parallel$ and αg_1^d are of considerable interest, both for testing the relativistic theory of the deuteron and for obtaining new information about the polarization structure of interacting particles, in particular, the neutron.

8. PRODUCTION OF CUMULATIVE SPECTATOR PROTONS ON THE DEUTERON

We now turn to strong interaction processes in which the deuteron participates. Of great interest here is the production of particles on the deuteron in the kinematic region forbidden in the approximation in which the deuteron consists of two practically free nucleons, i.e., the production of so-called cumulative particles. In the rest frame of the deu-

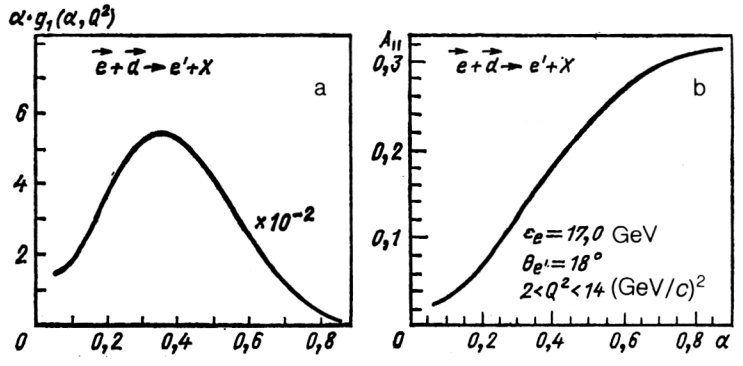

FIG. 18. Structure function αg_1^d (a) and asymmetry $A_\parallel$ (b) of the $\vec{e}\vec{d} \to e'X$ process in the impulse approximation [$\theta_{e'} = 18°$; $\varepsilon_e = 17.0$ GeV; $2 < Q^2 < 14$ $(\text{GeV}/c)^2$]. The continuous curves are the result of calculation with the wave function of Ref. 27.

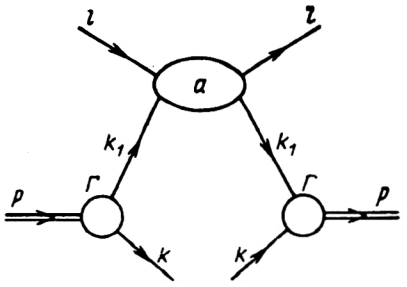

FIG. 19. Impulse approximation for inclusive production of a spectator nucleon on the deuteron.

teron, nucleons emitted in the backward hemisphere are cumulative. In the frame in which the deuteron moves rapidly, particles in its fragmentation region that carry away a large fraction of its longitudinal momentum are cumulative. In this section, we shall consider the production of cumulative nucleons. In contrast to other particles, pions and kaons, their production is not mainly as a result of the direct mechanism corresponding to the diagram shown in Fig. 4 but as a result of the observation of spectator nucleons. This corresponds to the six-point function shown in Fig. 19. We assume that averaging is performed over the spins of the incident particle, so that it can be regarded effectively as a scalar particle. Then the amplitude corresponding to the diagram in Fig. 19 can be represented in the form

$$A_{\alpha\beta}=\bar{u}(k)\bar{\psi}_\beta(k_1)a(l,k_1)\psi_\alpha(k_1)u(k). \tag{104}$$

Here, α and β are the vector indices of the deuteron; $u(\bar{u})$ describes the polarizations of the detected nucleon. The amplitude α describes the interaction of the incident particle with the active nucleon. Neglecting its virtuality in the region of high energies, we can describe it approximately by a formula analogous to (91):

$$a(l,k_1)=i\hat{l}\sigma^{\text{tot}}(s_1), \tag{105}$$

where $s_1=(l+k_1)^2$, σ^{tot} is the total cross section for interaction of the incident particle with the active nucleon, and we have assumed that at high energies the interaction amplitude is purely imaginary (the last assumption is not essential). Substituting (105) in (104), we contract $A_{\alpha\beta}$ with the polarization density matrix of the deuteron and sum over the polarizations of the spectator nucleon. Then, taking the absorptive part, we find the inclusive cross section for the production of an unpolarized spectator nucleon in the form

$$I_d^N(k)=k_0d^3\sigma/d^3k$$
$$=\sigma^{\text{tot}}(s_1)\ \text{Sp}\{\bar{\psi}_\beta(k_1)\hat{l}\psi_\alpha(k_1)(m+\hat{k})\}\rho^{\alpha\beta}/$$
$$2(pl)(2\pi)^3. \tag{106}$$

For an unpolarized deuteron, we must use the density matrix

$$\rho_{\alpha\beta}=-(g_{\alpha\beta}-p_\alpha p_\beta/M^2)/3. \tag{107}$$

Using the wave function $\psi_\alpha(k_1)$ constructed in Sec. 5, we calculated the inclusive cross section for production of spectators in the cumulative region of k values.

Figure 20 shows the dependence of the cross section I_d^p on the momentum k of a proton detected at angle θ_p. The experimental data are taken from Refs. 60 and 61. It can be seen from Fig. 20a that our calculation, both with allowance for the phase-space limit of the reation (continuous curve) and without it (broken curve), agrees qualitatively with the experimental data,[60] but both graphs lie somewhat above these data, a fact that we can attribute to the uncertainty in the absolute normalization. In Fig. 20b, our calculation is compared with the experimental data of Ref. 61. The arrow shows the kinematic limit of the reaction. It can be seen from Fig. 20b that there is good agreement between the calculation and the experiments far from

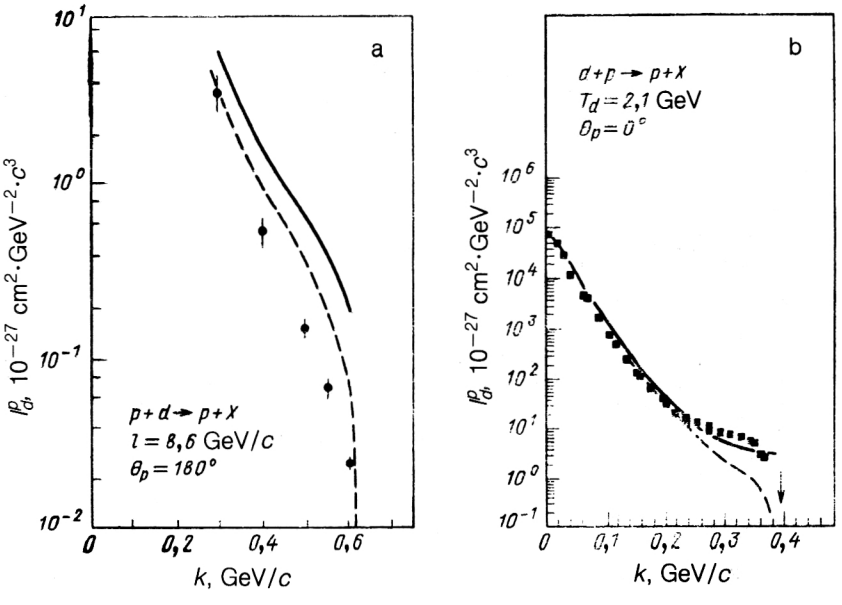

FIG. 20. Momentum spectra of protons in the reactions $pd\to pX$ (a) and $dp\to pX$ (b). The continuous curves are the results of calculations with the wave function of Ref. 27 without allowance for the kinematic limit of the reactions, and the broken curves take into account the kinematic limit. The experimental points are from Refs. 66 and 61.

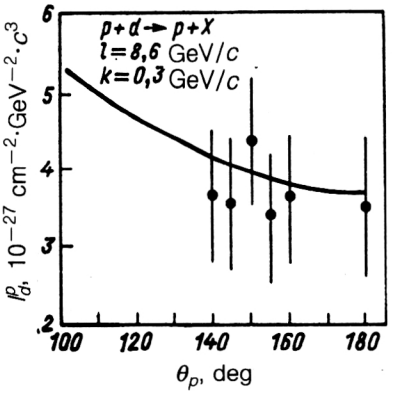

FIG. 21. Angular spectrum of protons in the $pd \to pX$ reaction. The continuous curve is the result of calculation of the contribution of the spectral mechanism with allowance for screening (factor ~ 0.8) and the phase-space limit of the reaction (Ref. 63); the experimental points are from Ref. 60.

the kinematic limit. In the cumulative region $k > 0.3$ GeV/c, the effect of the kinematic limit is important and prevents a direct comparison with experiment. With increasing energy of the incident deuteron, the kinematic limit is shifted to the right. The graph of the curve rises, and the discrepancy with the experimental data in the region $k > 0.3$ GeV/c must decrease.

Figure 21 gives a graph of the angular dependence of the spectrum of cumulative protons. It can be seen from the figure that the theoretical curve decreases monotonically with increasing angle θ_p and in the region $140 < \theta_p < 180°$ has a weak angular dependence. The same behavior is observed for the experimental data.[60]

It would be interesting to repeat the experiment of Ref. 60 with better statistics in the region $k > 0.1$ GeV/c in order to study the dependence of the cross section on the energy of the incident proton and the possibility of its factorization.

In the case of scattering by a tensor-polarized deuteron, the analyzing power T_{20} is defined as the mean value of the quadrupole part of the deuteron polarization density matrix, which has the form

$$\rho_{\alpha\beta}^{(T)} = S_{\alpha\beta}. \tag{108}$$

The tensor $S_{\alpha\beta}$ satisfies the conditions $S_{\alpha\beta} = S_{\beta\alpha}$, $S_{\alpha\alpha} = 0$, $p_\alpha S^{\alpha\beta} = 0$.

The tensor analyzing power T_{20} of the reaction $\vec{pd} \to pX$ is defined by

$$T_{20} = \frac{\sqrt{2}\,\mathrm{Sp}\{A^{zz}\rho_{zz}^{(T)}\}}{3\,\mathrm{Sp}\{A^{\alpha\beta}\rho_{\alpha\beta}\}}. \tag{109}$$

Figure 22a shows the dependence of T_{20} on the momentum k of a proton detected at angle θ_p. It can be seen from the figure that T_{20} at $\theta_p = 180°$ takes a negative value in the entire considered region of momenta and has characteristic behavior in the region $k \simeq 0.2$–0.4 GeV/c. Such behavior is due to the dynamic enhancement of the D wave in the deuteron. With increasing θ_p, the T_{20} curve has a tendency to rise and, beginning with a certain angle θ_p^* it intersects the k axis and becomes positive.

Figure 22b shows the results of our calculation of T_{20} in the impulse approximation in the kinematics of the Saclay experiment of Ref. 61. It can be seen that there is qualitative agreement between the theoretical curve and the data of Ref. 61. In our opinion, the difference is due to the contribution of the mechanisms that lead to the excess in the reaction cross section. In a number of studies, it is attributed to the effect of the pion enhancement associated with rescattering[64] and absorption,[65] and also a contribution of a six-quark state in the deuteron.[63]

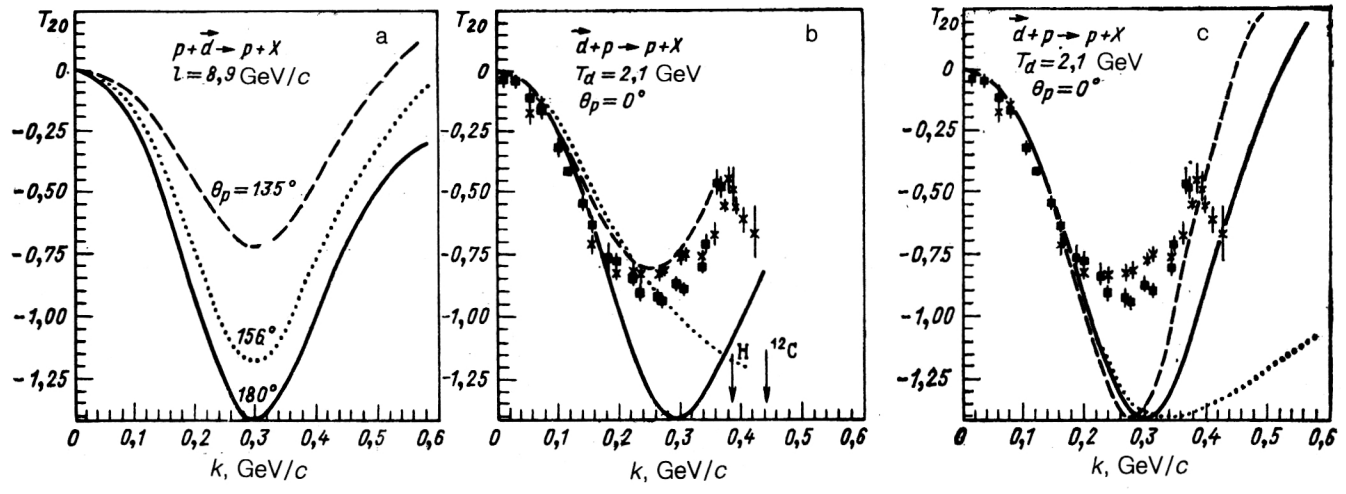

FIG. 22. Momentum spectra of tensor analyzing power T_{20} of the reactions $\vec{pd} \to pX$ (a) and $\vec{dp} \to pX$ (b, c): a) the broken, dotted, and continuous curves are the results of calculations for different emission angles of the spectator nucleon; b) the continuous and dotted curves are the results of calculations with a deuteron wave function with a core[27] and without it,[26] and the broken curve is a phenomenological calculation with normalization to the experimental cross section; c) the continuous, dotted, and broken curves are the results of calculation in accordance with the expression (110) with the relativistic deuteron wave functions of Refs. 27, 26, and 19, respectively.

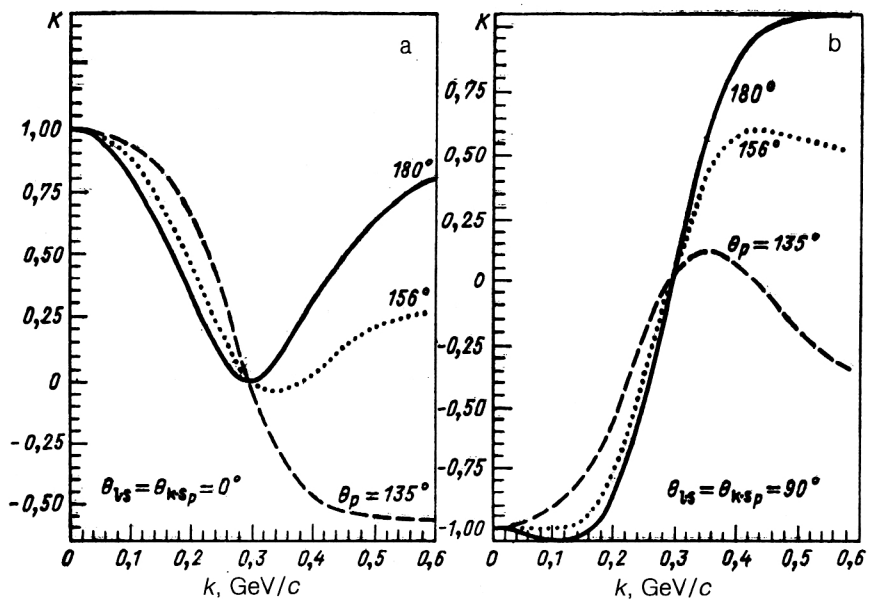

FIG. 23. Vector polarization-transfer coefficients of the $\vec{pd}\to\vec{p}X$ process in the impulse approximation ($l=8.9$ GeV/c). The broken, dotted, and continuous curves are the results of calculations with the relativistic deuteron wave function of Ref. 27 for various emission angles of the spectator nucleon.

In Fig. 22b, the broken curve is a calculation with phenomenological allowance for the excess. It can be seen that it agrees well with the experiment of Ref. 61. For complete description of these data in the framework of the covariant approach in light-cone variables, calculations of the mechanisms noted in Refs. 64 and 65 would be interesting.

It should be noted that the nonrelativistic calculation of Ref. 66 with allowance for pion enhancement makes it possible to describe the data on T_{20} in the region of the minimum. In the high-momentum region $k>0.4$ GeV/c, the graph of T_{20} enters the region of positive values and does not describe these data even qualitatively.

Figure 22c shows the results of calculation of T_{20} determined by the nonrelativistic formula

$$T_{20}=2(\sqrt{2}uw-w^2)/\sqrt{2}(u^2+w^2) \qquad (110)$$

with three relativistic deuteron wave functions.

Calculations with relativistic deuteron wave functions[19,27] having a core lead to qualitatively similar results and differ appreciably from the calculation with the relativistic wave function of Ref. 26 without a core in the region $k>0.3$ GeV/c.

In the reaction $\vec{pd}\to\vec{p}X$, polarization is transferred from the vector-polarized deuteron to the detected polarized proton. The transfer is characterized by a vector polarization-transfer coefficient K, which is the mean value with respect to the deuteron of the vector part of the deuteron polarization density matrix for polarized protons. In this case, the density matrix has the form

$$\rho^{(V)}_{\alpha\beta}=i\varepsilon_{\alpha\beta\mu\nu}s^\mu p^\nu/2M. \qquad (111)$$

We define the vector polarization-transfer coefficient by

$$K=\frac{\mathrm{Sp}\{\bar{\psi}^\beta(k_1)l\hat{\psi}^\alpha(k_1)\gamma_5\hat{s}_p(m+\hat{k})\rho^{(V)}_{\alpha\beta}\}}{\mathrm{Sp}\{A^{\alpha\beta}\rho_{\alpha\beta}\}}, \qquad (112)$$

where s_p and s are the polarization vectors of the proton and deuteron. They satisfy the conditions $s^2=s_p^2=-1$, $(ps)=0$, $(ks_p)=0$.

Figure 23 gives the results of calculation of the coefficient K as a function of the proton momentum k for angles θ_p equal to 135, 156, 180°. Figure 23a shows the case when the polarization vectors $\mathbf{s}$ and $\mathbf{s}_p$ are parallel and make an angle 0° with the momenta of the corresponding particles, while in Fig. 23b they make an angle 90°. As can be seen from the figure, a characteristic feature of the curves is that at $k=0.3$ GeV/c they pass through zero. This may mean that the vector polarization-transfer coefficients, in contrast, for example, to T_{20}, are determined in the region $k\simeq 0.3$ GeV/c by the S-wave function of the deuteron. One may suppose that the effect that arises from the mechanisms responsible for the excess in the cross section is small for the vector polarization-transfer coefficients.

We do not possess experimental information for K, and therefore the calculations are predictive in nature.

Hitherto, we have considered the production of cumulative spectator nucleons in deuteron–proton interactions. However, as is clear from the form of the diagram in Fig. 19 and Eq. (106), our results depend on the type of incident particle only through the total cross section σ^{tot}. Therefore, the foregoing analysis can be directly generalized to processes of fragmentation of a fast deuteron with nuclei of the type $dA\to pX$. All the expressions are unchanged except that the NN scattering cross section σ^{tot} must be replaced by the NA scattering cross sections $\sigma^{\mathrm{tot}}_{NA}$.

Figure 24a shows the result of calculation of the dependence of the fragmentation cross section I^p_d and the tensor analyzing power T_{20} of the $d^{12}\mathrm{C}\to pX$ reaction on the momentum of the detected proton obtained in the framework of the covariant formalism with a relativistic deuteron wave function in light-cone variables with one nucleon and the deuteron on the mass shell. The experi-

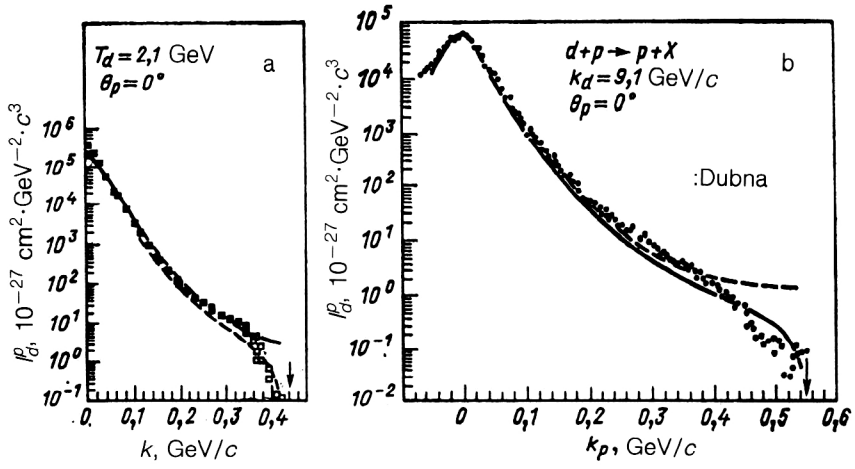

FIG. 24. Invariant cross section of the $d^{12}C \to pX$ reaction in the impulse approximation. The continuous and broken curves are the results of calculations with the relativistic deuteron wave function of Ref. 27 without allowance and with allowance for the kinematic limit of the reaction, respectively. The experimental points are taken from Ref. 61.

mental data are taken from Ref. 61.

As can be seen from Figs. 24 and 20, the results of the calculation for the $d^{12}C \to pX$ reaction are qualitatively similar to the results of the calculation for the $dp \to pX$ reaction. Note that the kinematic limit for the $d^{12}C \to pX$ reaction is shifted to the right, and therefore in the region of the excess the effect of the kinematic limit is not manifested so strongly as for the $dp \to pX$ reaction.

In Fig. 24b, our calculation is compared with the experiment of Ref. 67. The continuous curve is the calculation with allowance for the kinematic limit of the reaction, while the broken curve is without allowance for it. The kinematic limit is indicated in Fig. 24b by the arrow. In the kinematics of the experiment of Ref. 67 the reaction limit is shifted to the right compared with the experiment of Ref. 61, and the region of the excess is clearly seen: $0.2 \leqslant k < 0.4$ GeV/c. These data are particularly interesting for estimating the contribution of the mechanism of resonant pion enhancement, since the influence of the kinematic limit is here unimportant.

In Fig. 25a, our calculation of T_{20} is compared with the experiment of Ref. 67. It can be seen from Fig. 25b that phenomenological allowance for the excess gives a good description of the experimental data. This result suggests that it is important to take into account nonspectator diagrams only in the cross section I_d^p in the calculation of T_{20}.

A further question on which we should like to dwell is the possibility of factorization of the cross section and the tensor analyzing power. Factorization means that a cross section or other dynamical characteristic of the process (for example, T_{20}) of interaction of the particle h with the nucleus A can be represented as a product of the cross section for interaction of the particle h with a nucleon of the nucleus and a function that describes the momentum distribution of the nucleons in the nucleus. In the case of nonrelativistic motion of the nucleons in the nucleus (k

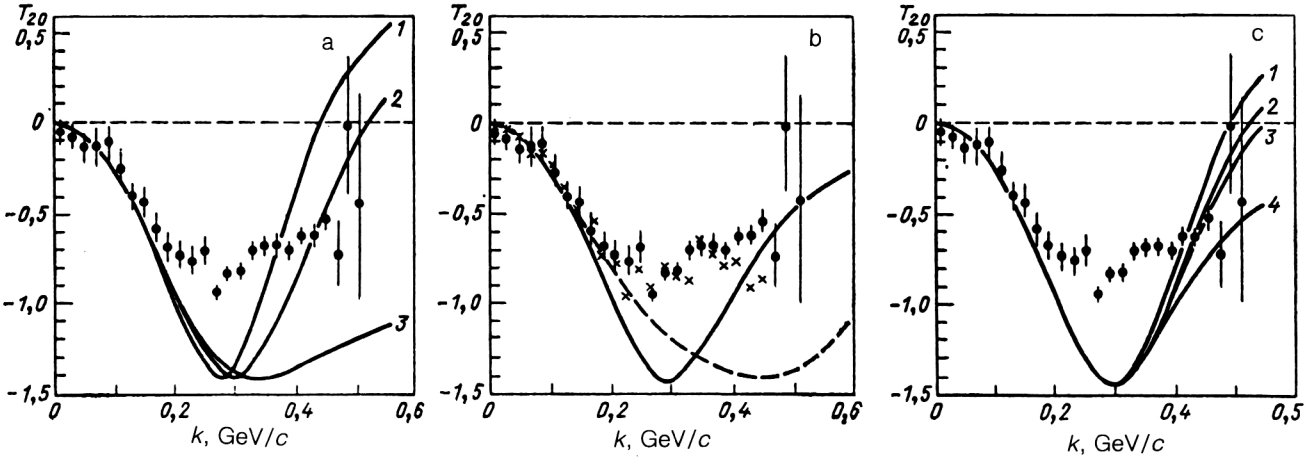

FIG. 25. Tensor analyzing power T_{20} of the reaction $\vec{d}p \to pX$ ($p_d = 9.1$ GeV/c, $\theta_p = 0°$). The experimental points are from Ref. 67: (a) 1), 2), 3) calculations in accordance with the expression (110) with relativistic wave functions of Refs. 19, 27, and 26, respectively; (b) the continuous curve is the result of calculation of T_{20} in accordance with the expression (109) with relativistic deuteron wave functions with a core from Ref. 27; the broken curve is the same but without a core from Ref. 26; the crosses represent calculation with the wave function of Ref. 27 but with normalization to the experimental cross section; (c) 1), 2) nonrelativistic and 3) relativistic calculations with wave functions of Refs. 34, 27 and 27, respectively, and with the assumption of factorization of I_d^p and T_{20}; 4) relativistic calculation with the wave function of Ref. 27 without the assumption of factorization.

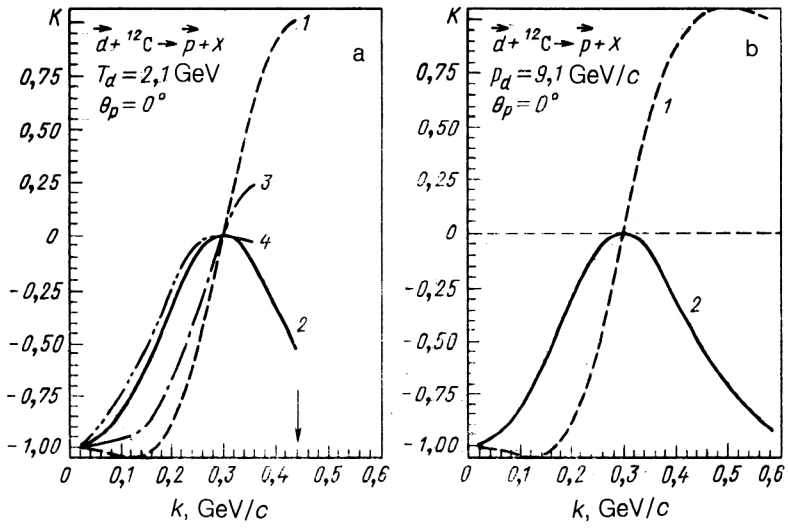

FIG. 26. Vector polarization-transfer coefficients of the $\vec{d}^{12}C \to \vec{p}X$ process in the impulse approximation (see the text for the notation).

< 100 MeV/c), such an assumption is justified, but it may not be so in the relativistic region.[30]

It can be seen from Fig. 25c that a significant difference in the behavior of all the curves is observed for $k > 0.3$ GeV/c. Curve 4 gives a good qualitative description of the experimental data. The absence of factorization in the relativistic region gives a larger effect than the relativization of the wave function. A result similar to curve 2 was obtained in Ref. 66, but that study used a different method of relativization and took into account a complex $6q$-component wave function of the deuteron. For the last assumption it is difficult to give any physically reasonable motivation.

Thus, for consistent description of the $dA \to pX$ reaction in the framework of the covariant approach in light-cone variables it is necessary to take into account, besides the spectator mechanism, other reaction mechanisms, for example, rescattering and absorption of a pion with allowance for the factorization effect.

Figure 26 gives the results of calculation of the vector polarization-transfer coefficients K of the $\vec{d}^{12}C \to \vec{p}X$ reaction for two cases of kinematics: Saclay (a) and Dubna (b). In the first (curves 1 and 3) it was assumed that $\theta_{ps} = 90°$, $\theta_{ks_p} = 90°$, and in the second (curves 2 and 4) $\theta_{ps} = 0°$, $\theta_{ks_p} = 0°$. Curves 1, 2 and 3, 4 were obtained without and with phenomenological allowance for the excess in the reaction cross section, respectively. The arrow indicates the kinematic limit of the reaction. These calculations are predictions and are of interest for experimental verification.

9. PRODUCTION OF CUMULATIVE PIONS AND KAONS ON DEUTERONS

Production of cumulative pions and kaons can occur as a result of both the direct mechanism[68] and the rescattering mechanism.[69] The first is associated with production of a cumulative particle on one of the nucleons of the nucleus with a large Fermi momentum. Its contribution is determined by the high-momentum component of the relativistic deuteron wave function. The second mechanism involves both nucleons in the production of the cumulative particle and does not depend on the presence of the high-momentum component.

The description of the $pd \to hX$ process is similar for π^+ and K^+ mesons. Therefore, in what follows we shall consider in most detail the $pd \to \pi^+ X$ reaction.

The production of cumulative pions on the deuteron at large angles occurs mainly through the direct mechanism, although rescattering does make a certain contribution. We shall consider only the contribution of the direct mechanism, which can be expressed in terms of the inclusive cross section for pion production on a nucleon, integrated over x and $k_\perp$ with the relativistic deuteron wave function.

The direct mechanism is represented by the diagram in Fig. 4a and the corresponding formula (30), which merely needs to be generalized to the case of nonvanishing spins. As the deuteron wave function there appears $\psi_\alpha(k_1)$, and from the spectator nucleon there remains a factor $(m + \hat{k})$. The inclusive cross section on the constituent active nucleon is multiplied by the factor $\hat{l}/s$, which has the same origin as the factor $\hat{l}/2(pl)$ in Eq. (106). Finally, the vector indices of the deuteron must be contracted with its polarization density matrix $\rho_{\alpha\beta}$. The upshot is that we find, in place of (30),

$$I_d^h(s,\alpha,r_\perp) = \int_0^{1-\alpha} \frac{dx}{2x} \int \frac{d^2k_\perp}{(2\pi)^3} \times I_N^h[s(1-x),\alpha/(1-x),r'_\perp] \times \mathrm{Sp}\{\bar{\psi}_\beta(k_1)\hat{l}\psi_\alpha(k_1)(m+\hat{k})\}\rho^{\alpha\beta}/s. \quad (113)$$

The connection between the variables k_1^2 and r'_1 and the variables of integration is still given by (21) and (31). The quantity I_N^h is the inclusive cross section for particle production on an unpolarized nucleon.

Substituting the deuteron wave functions ψ_α constructed in Sec. 5 and the experimentally known inclusive cross sections for production of pions on the proton and

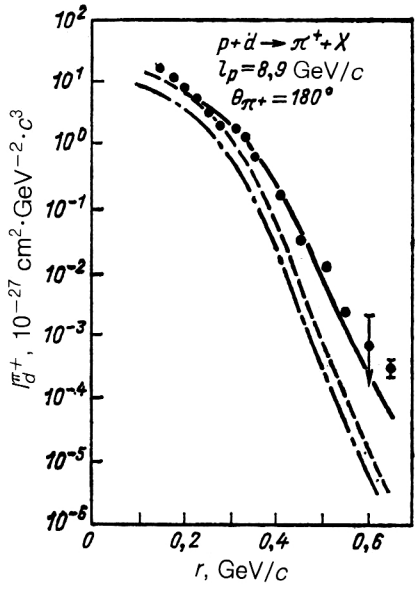

FIG. 27. Momentum spectrum of cumulative pions in the $pd \to \pi^+ X$ reaction.

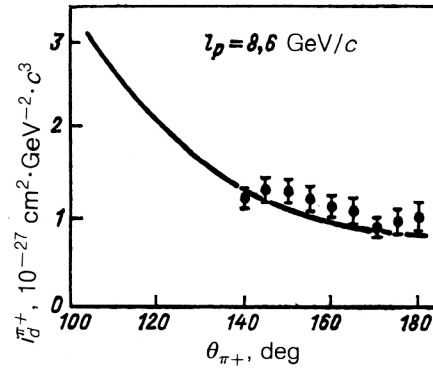

FIG. 28. Angular spectrum of cumulative pions in the $pd \to \pi^+ X$ reaction. The continuous curve is the result of calculation with $I_p^{\pi^+}$ from Ref. 71; the experimental points are from Ref. 60.

neutron, we find from (113) the inclusive cross sections for production on the deuteron.

Figure 27 shows the results of our calculation of the spectrum of cumulative pions emitted in the backward hemisphere, $\theta_{\pi^+} = 180°$. The continuous, broken, and chain curves in Fig. 27 correspond to choice of the parametrization of the inclusive cross sections $I_p^{\pi^+}$ in the form

$$I_p^{\pi^+}(x,k_\perp) = 75.1[1 - 0.897x/(1 + 0.103x/2)]^{3.3} \times (1-x)^{0.2}; \quad (114)$$

$$I_p^{\pi^+}(x,k_\perp) = 30.2(1-x)^{3.2}(1 + k_\perp^2/0.66)^{-4}; \quad (115)$$

$$I_p^{\pi^+}(x,k_\perp) = 60.2(1-x)^{3.4}\exp(-4{,}1k_\perp), \quad (116)$$

which are taken from Refs. 70–72, respectively. In all cases, it was assumed that $I_N^{\pi^+} = I_p^{\pi^+}[1 + f(x)]/2$ and $f(x) = 0.3\exp(-0.51x)$. The experimental points are taken from Ref. 73. It can be seen from Fig. 27 that the spectrum of cumulative pions depends strongly on the behavior of the cross section $I_p^{\pi^+}$ in the region $x \simeq 1$. The choice of $I_p^{\pi^+}$ in the form (114) makes it possible to achieve a good description of the experimental data. We attribute this result to enhancement of the Fermi motion of the nucleons in the deuteron through the relativistic off-shell effect. The two other curves do not describe the experimental data, and in the region $r > 0.4$ GeV/c they are too low by more than an order of magnitude.

Figure 28 shows the graph of the angular dependence of the spectrum of cumulative pions at $r_{\pi^+} = 0.3$ GeV/c. The theoretical curve decreases monotonically with increasing pion emission angle and reaches a minimum at $\theta_{\pi^+} = 180°$. The experimental points[60] lie somewhat above the curve, but their behavior does not exhibit significant qualitative differences. Both the experimental points and the curve indicate a weak angular dependence in the production of cumulative pions at large angles ($\theta_{\pi^+} > 140°$). One may conclude that the contribution to the cross section of the rescattering mechanism is not too large at $\theta_{\pi^+} = 180°$.

In conclusion, we consider the production of cumulative π^+ and K^+ mesons by protons on a tensor-polarized deuteron.

In accordance with our expressions, the tensor analyzing power of the $\vec{pd} \to hX$ reaction is determined by

$$T_{zz(xx)} = t_d^h(s,\alpha,r_\perp)/I_d^h(s,\alpha,r_\perp), \quad (117)$$

where

$$t_d^h(s,\alpha,r_\perp) = \int_0^{1-\alpha} dx \int d^2k_\perp I_N^h(s(1-x),\alpha/ \times (1-x),r_\perp')\Phi^{zz(xx)}(x,k_\perp)S_{zz(xx)}.$$

Here, $S_{zz(xx)}$ is the component of the quadrupole part of the polarization density matrix, and Φ is a known function that is determined by the structure of the relativistic deuteron wave function.

Figures 29 and 30 give the results of our calculation of the spectra of cumulative π^+ and K^+ emitted at angle $\theta_h = 180°$, and also the tensor analyzing powers of the $pd \to (\pi^+,K^+)X$ reaction. In the calculations for $I_p^h(x,k_\perp)$ we used the parametrizations from Ref. 74, and we also assumed $I_N^h = I_p^h$. The last assumption does not significantly influence the qualitative behavior of I_d^h, which is more sensitive to the behavior of I_p^h in the region $x \simeq 1$. It can be assumed that T_{zz} and T_{xx} depend weakly on the normalization of the cross section.

It can be seen from Fig. 29 that the I_d^h curves for the relativistic deuteron wave function with a core[27] and without a core[26] are practically coincident for π^+ in the region $r < 0.5$ GeV/c and for K^+ in the region $r < 0.3$ GeV/c. At large momenta of the cumulative particles, the curves calculated using the wave function with a core lie below the corresponding curves for the wave function without a core.

The behavior of T_{zz} and T_{xx} for π^+ in the region $r < 0.45$ GeV/c depends weakly on the deuteron wave function in the region of the core. For $r > 0.45$ GeV/c, a sig-

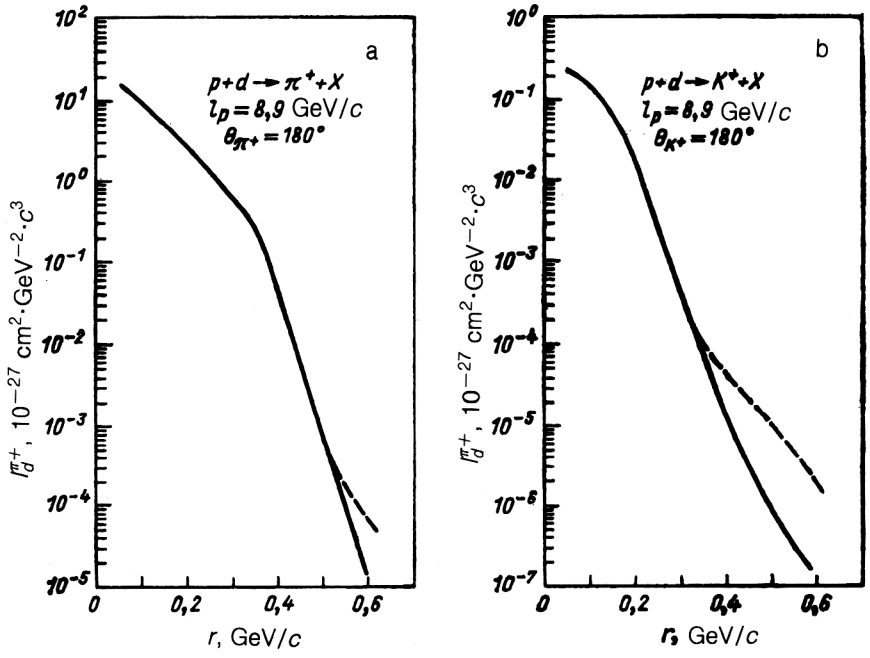

FIG. 29. Momentum spectrum of cumulative pions (a) and kaons (b) in the $pd\to hX$ reaction in the impulse approximation. The continuous and broken curves are the results of calculations with a deuteron wave function with a core[27] and without a core,[26] respectively.

nificant qualitative and quantitative difference is observed. It can be seen from Fig. 30a that the T_{zz} curve with the wave function of Ref. 26 in the region $0.4 < r < 0.55$ GeV/c lies above the curve calculated with the wave function of Ref. 27. The behavior of T_{xx} in the region $r < 0.3$ GeV/c is almost independent of the form of the deuteron wave function, while for $r > 0.3$ GeV/c an appreciable difference in the behavior of these functions is observed.

The calculated results show that an experiment to measure the tensor analyzing power of the $\vec{pd} \to (\pi^+, K^+)X$ process can give new information about the structure of the relativistic deuteron wave function in the region of the core.

It can be seen from Fig. 30 that with increasing mass of the produced cumulative particle h the graphs of the dependences of I_h^d, T_{zz}, T_{xx} have a tendency to move into the region of smaller momenta r.

Figure 31 shows the results of our calculation of the angular dependences of the tensor analyzing powers of the $\vec{pd} \to (\pi^+, K^+)X$ reaction in the impulse approximation with the relativistic deuteron wave function of Ref. 27.

Ratio of yields of π^+ and K^+ mesons in the $pd\to hX$ reaction

The interest in study of the yields of π^+ and K^+ mesons on nuclei in the cumulative region is due to the assertion that in the cumulative region there is an enhancement of the production of sea cumulative particles, and the ratio $R^{\pi^+/K^+} \sim 1$ observed in the experiment of Ref. 76 was attributed to a harder than expected structure function of the sea quarks.

Figure 32 shows a graph of the ratio $R^{\pi^+/K^+} = I_d^{\pi^+}(180°)/I_d^{K^+}(180°)$ as a function of the variable x (Ref. 75).

In Ref. 77, the dependence of R^{π^+/K^+} was investigated in the framework of the flucton model of the nucleus. Our calculation of R^{π^+/K^+} obtained without explicit inclusion of quarks (continuous curve in Fig. 32) differs appreciably from the behavior of R^{π^+/K^+} obtained in Ref. 77 but is qualitatively similar to the behavior of this ratio obtained in Ref. 77 with allowance for quark degrees of

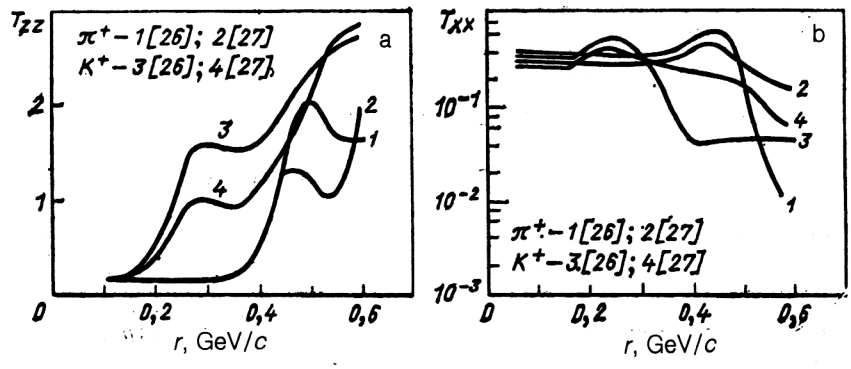

FIG. 30. Tensor analyzing powers T_{zz} (a) and T_{xx} (b) of the reaction $\vec{pd}\to hX$ ($h = \pi^+, K^+$) in the impulse approximation ($l_p = 8.9$ GeV/c) (references are given in square brackets).

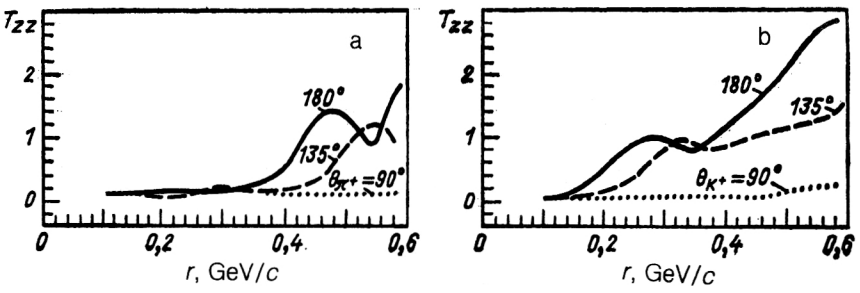

FIG. 31. Momentum dependences of the tensor analyzing power T_{zz} of the $\vec{pd}\to hX$ reaction for pions (a) and kaons (b) with $l_p = 8.9$ GeV/c. The dotted, broken, and continuous curves are the results of calculations with the wave function of Ref. 27 for angles θ_h equal to 90, 135, 180°.

freedom in the framework of the fluctron model. In Fig. 32, the broken curve shows our calculation of R^{π^+/K^+} with the deuteron wave function without a core from Ref. 26. It can be seen from Fig. 32 that the behavior of R^{π^+/K^+} in the region $1.1 < x < 1.6$ is determined by the structure of the wave function in the region of the core. For $x < 1.1$ and $x > 1.6$ the graphs of the ratio R^{π^+/K^+} obtained with the wave function of Ref. 27 with a core and with the wave function of Ref. 26 without a core are practically identical.

Note that in the considered region $0 < x < 2$ the ratio is $R^{\pi^+/K^+} \sim 3$–11, and this is basically in agreement with the results obtained in Ref. 77.

CONCLUSIONS

In this review, we have given a description of the relativistic deuteron in terms of a relativistic wave function with one nucleon on the mass shell and of processes with its participation in the framework of a covariant approach in light-cone variables.

Combination of the manifestly covariant description with the advantage of using a distinguished frame of reference has made it possible to approach constructively the problem of constructing a relativistic deuteron wave function, and the use of the Bethe–Salpeter function restricted in virtuality with one of the nucleons on the mass shell has made it possible to reduce the number of independent relativistic wave functions and to establish with less uncertainty the structure of the components of the wave function in the relativistic region.

The scheme proposed for constructing a relativistic deuteron wave function, or relativization scheme, which has as its nonrelativistic limit the well-known nonrelativistic wave function, differs from the one usually adopted and does not reduce to formal replacement of the argument of the nonrelativistic wave function.

Systematic analysis, in the framework of the unified approach, of a large number of processes involving polarized and unpolarized deuterons suggests that the covariant approach in light-cone variables gives an adequate description of these processes and is very promising. It can be used for the relativistic description of three- and four-nucleon systems, although the difficulties then increase appreciably.

From the point of view of practical applications, the constructed relativistic deuteron wave functions can be used for a relativistic description of processes with electromagnetic, weak, and strong interaction, and also to analyze experimental data on processes involving deuterons in existing and planned investigations at the JINR, IHEP, Leningrad Institute of Nuclear Physics, the Institute of Nuclear Physics, the Khar'kov Physicotechnical Institute (USSR), SLAC, SEBAF (USA), Saclay (France), and elsewhere.

The actual predictions for a number of processes made in the framework of this approach are of interest both for experimental verification and for comparison with the results obtained in the framework of other relativistic approaches, and this should stimulate the further development of the relativistic theory of nuclear systems.

The currently observed significant progress in the creation of polarized beams of particles of high and superhigh energies in the largest laboratories in the world is raising relativistic nuclear physics to a qualitatively new level of development, where, we hope, the relativistic theory of nuclear systems will make contact with the fundamental theory of the strong interactions: QCD.

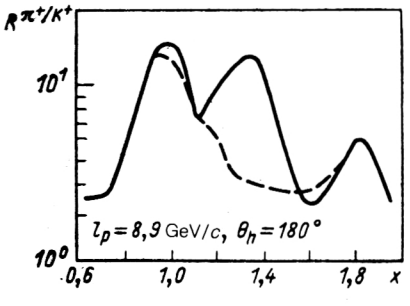

FIG. 32. Ratio R^{π^+/K^+} of yields of π^+ and K^+ mesons in the $pd\to hX$ reaction. The continuous and broken curves are the results of calculations with the wave functions of Refs. 27 and 26, respectively.

[1] E. E. Salpeter and H. A. Bethe, Phys. Rev. **84**, 1232 (1951).
[2] R. Blankenbecler and L. F. Cook, Phys. Rev. **119**, 1745 (1960).
[3] A. A. Logunov and A. N. Tavkhelidze, Nuovo Cimento **29**, 370 (1963).
[4] V. G. Kadyshevsky, Nucl. Phys. **6**, 125 (1968).
[5] F. Gross, Phys. Rev. **186**, 1448 (1969).
[6] S. J. Brodsky and G. P. Lepage, Phys. Rev. D **22**, 2157 (1980).
[7] A. I. Kirillov, V. E. Troitskiĭ, S. V. Trubnikov, and Yu. M. Shirokov, Fiz. Elem. Chastits At. Yadra **6**, 3 (1975) [Sov. J. Part. Nucl. **6**, 1 (1975)].
[8] V. M. Muzafarov, V. E. Troitskiĭ, and S. V. Trubnikov, Fiz. Elem. Chastits At. Yadra **14**, 1112 (1983) [Sov. J. Part. Nucl. **14**, 467 (1983)].
[9] V. A. Karmanov, Zh. Eksp. Teor. Fiz. **75**, 1187 (1978) [Sov. Phys. JETP **48**, 598 (1978)].
[10] V. A. Karmanov and I. S. Shapiro, Fiz. Elem. Chastits At. Yadra **9**, 327 (1978) [Sov. J. Part. Nucl. **9**, 134 (1978)].
[11] V. A. Karmanov, Fiz. Elem. Chastits At. Yadra **19**, 525 (1988) [Sov. J.

Part. Nucl. **19**, 228 (1988)].
[12] M. I. Strikman and L. L. Frankfurt, Fiz. Elem. Chastits At. Yadra **11**, 571 (1980) [Sov. J. Part. Nucl. **11**, 221 (1980)].
[13] L. L. Frankfurt and M. I. Strikman, Phys. Rep. **76C**, 215 (1981); Phys. Rep. **160**, 235 (1988).
[14] L. A. Sliv, M. I. Strikman, and L. L. Frankfurt, Usp. Fiz. Nauk **145**, 552 (1985) [Sov. Phys. Usp. **28**, 281 (1985)].
[15] S. J. Brodsky and G. R. Farrar, Phys. Rev. D **11**, 1309 (1975).
[16] B. L. G. Bakker, L. A. Kondratyuk, and M. V. Terent'ev, Nucl. Phys. **B158**, 497 (1979).
[17] P. V. Landshoff, J. C. Polkinghorne, and R. D. Short, Nucl. Phys. **B28**, 225 (1971).
[18] F. Gross, Phys. Rev. D **10**, 223 (1974).
[19] W. W. Buck and F. Gross, Phys. Rev. D **20**, 2361 (1979).
[20] R. G. Arnold, C. E. Carlson, and F. Gross, Phys. Rev. C **21**, 1426 (1980).
[21] R. G. Arnold, C. E. Carlson, and F. Gross, Phys. Rev. C **23**, 363 (1981).
[22] M. A. Braun, Yad. Fiz. **32**, 1283 (1980) [Sov. J. Nucl. Phys. **32**, 662 (1980)].
[23] M. I. Strikman and L. L. Frankfurt, Yad. Fiz. **27**, 1361 (1978) [Sov. J. Nucl. Phys. **27**, 717 (1978)].
[24] M. V. Terent'ev, Yad. Fiz. **24**, 207 (1976) [Sov. J. Nucl. Phys. **24**, 106 (1976)].
[25] M. A. Braun, Yad. Fiz. **42**, 818 (1985) [Sov. J. Nucl. Phys. **42**, 518 (1985)].
[26] M. A. Braun and M. V. Tokarev, Vestn. Leningr. Univ. No. 22, 6 (1983).
[27] M. A. Braun and M. V. Tokarev, Vestn. Leningr. Univ. Ser. 4, No. 1, 7 (1986).
[28] M. A. Braun and M. V. Tokarev, Vestn. Leningr. Univ. No. 22, 66 (1984).
[29] M. A. Braun and M. V. Tokarev, in *Nucleon–Nucleon and Hadron–Nucleus Interactions at Intermediate Energies. Proc. of the Third Symposium of the Leningrad Institute of Nuclear Physics* [in Russian] (publishing house of the Leningrad Institute of Nuclear Physics, Leningrad, 1986), p. 311.
[30] M. V. Tokarev, *Few-Body Systems*, Vol. 4 (1988), p. 133.
[31] M. A. Braun and M. V. Tokarev, in *Pion–Nucleon and Nucleon–Nucleon Physics. Proc. of the Third International Symposium* (publishing house of the Leningrad Institute of Nuclear Physics, Leningrad, 1989), p. 398.
[32] M. V. Tokarev, "Relativistic description of the deuteron in the framework of a covariant formalism in light-cone variables," Candidate's Dissertation [in Russian], Tashkent (1987).
[33] M. Gourdin, M. Le Bellac, F. M. Renard *et al.*, Nuovo Cimento **37**, 524 (1965).
[34] M. Lacombe, B. Loiseau, and R. Vinh Mau, Phys. Lett. **101B**, 139 (1981).
[35] I. J. McGee, Phys. Rev. **151**, 772 (1966).
[36] A. P. Kobyshkin and V. P. Shelest, Fiz. Elem. Chastits At. Yadra **14**, 1146 (1983) [Sov. J. Part. Nucl. **14**, 483 (1983)].
[37] A. B. Migdal, Pis'ma Zh. Eksp. Teor. Fiz. **46**, 256 (1987) [JETP Lett. **46**, 280 (1988)]; *Proc. of the Ninth International Seminar on High Energy Physics Problems* (Dubna, June 14–19, 1988), p. 38.
[38] S. Galster, H. Klein, J. Moritz *et al.*, Nucl. Phys. **32**, 221 (1971).
[39] F. Jachello, A. D. Jackson, and A. Lande, Phys. Lett. **43B**, 191 (1973).
[40] A. I. Akhiezer and M. P. Rekalo, *Electrodynamics of Hadrons* [in Russian] (Naukova Dumka, Kiev, 1979).
[41] P. S. Isaev, *Quantum Electrodynamics at High Energies* (AIP, New York, 1989) [Russ. original], Énergoatomizdat, Moscow, 1984.
[42] V. Glaser and B. Jakŝic, Nuovo Cimento **5**, 1197 (1957).
[43] H. F. Jones, Nuovo Cimento **26**, 790 (1962).
[44] M. Gourdin, Nuovo Cimento **28**, 534 (1963).
[45] R. G. Arnold, B. Chertok, E. Dally *et al.*, Phys. Rev. Lett. **35**, 776 (1975).
[46] R. G. Arnold, B. Chertok, B. A. Mecking *et al.*, *Proc. of the Ninth ICOHEPANS. Abstracts of Contributed Papers* (1981), p. 94.
[47] R. Cramer, M. Renkhoff, J. Drees *et al.*, Z. Phys. C **25**, 513 (1985).
[48] M. J. Zuilhof and J. A. Tjon, Phys. Rev. C **22**, 2369 (1980).
[49] S. Auffret, J. M. Covedon, J. C. Clemens *et al.*, Phys. Rev. Lett. **54**, 649 (1985).
[50] R. G. Arnold, D. Benton, P. Bosted *et al.*, Phys. Rev. Lett. **58**, 1723 (1987).
[51] M. E. Schulze, D. Beck, M. Farkhoudeh *et al.*, Phys. Rev. Lett. **52**, 587 (1985).
[52] D. K. Vesnovskiĭ, B. B. Voĭtsekhovskiĭ, V. F. Dmitriev *et al.*, Preprint 86-75 [in Russian], Institute of Nuclear Physics, Novosibirsk (1986).
[53] F. E. Close, *An Introduction to Quarks and Partons* (Academic Press, London, 1979) [Russ. transl., Mir, Moscow, 1982].
[54] V. V. Burov, V. K. Luk'yanov, and A. I. Titov, Fiz. Elem. Chastits At. Yadra **15**, 1249 (1984) [Sov. J. Part. Nucl. **15**, 558 (1984)].
[55] W. P. Shütz, R. G. Arnold, B. T. Chertok *et al.*, Phys. Rev. Lett. **38**, 259 (1977).
[56] D. W. Duke and J. F. Owens, Phys. Rev. D **30**, 49 (1984).
[57] A. Bodek, M. Briedenbach, D. L. Dubme *et al.*, Preprint SLAC–PUB. 2248 (1979).
[58] J. Kaur, Nucl. Phys. **B128**, 219 (1977); R. Carlitz and J. Kaur, Phys. Rev. Lett. **38**, 673 (1977).
[59] J. Ashman, B. Badelek, G. Baum *et al.*, Phys. Lett. **206B**, 364 (1988).
[60] A. M. Baldin, V. K. Bondarev, L. B. Golovanov *et al.*, Preprint R1-11168 [in Russian], JINR, Dubna (1977).
[61] C. F. Perdrisat, A. Punjaudard, C. Lyndon *et al.*, Phys. Rev. Lett. **59**, 2840 (1987).
[62] L. L. Frankfurt and M. I. Strikman, Nucl. Phys. **A405**, 557 (1983).
[63] V. G. Ableev, A. A. Abdushukurov, S. A. Avramenko *et al.*, Nucl. Phys. **A393**, 491 (1983).
[64] M. A. Braun and V. V. Vechernin, Yad. Fiz. **43**, 1579 (1986) [Sov. J. Nucl. Phys. **43**, 1016 (1986)].
[65] M. A. Ignatenko and G. I. Lykasov, Yad. Fiz. **46**, 1080 (1987) [Sov. J. Nucl. Phys. **46**, 625 (1987)].
[66] M. G. Dolidze and G. I. Lykasov, Preprint E2-89-666, JINR, Dubna (1989).
[67] V. G. Ableev, S. V. Dshemuchadze, S. V. Fedukov *et al.*, Preprint E1-88-250, JINR, Dubna (1988); V. G. Ableev, L. Vizireva, V. I. Volkov *et al.*, Pis'ma Zh. Eksp. Teor. Phys. **47**, 558 (1988) [JETP Lett. **47**, 649 (1988)]; V. G. Ableev, S. V. Dshemuchadze, S. V. Fedukov *et al.*, Rapid Communication, No. 4[43]-90, JINR, Dubna (1990), p. 5.
[68] G. A. Lobov, V. E. Markushin, V. V. Solov'ev, and I. S. Shapiro, Pis'ma Zh. Eksp. Teor. Fiz. **23**, 118 (1976) [JETP Lett. **23**, 102 (1976)]; S. I. Strikman and L. L. Frankfurt, Pis'ma Zh. Eksp. Teor. Fiz. **24**, 311 (1976) [JETP Lett. **24**, 279 (1976)].
[69] L. A. Kondratyuk and V. B. Kopeliovich, Pis'ma Zh. Eksp. Teor. Fiz. **21**, 88 (1975) [JETP Lett. **21**, 40 (1975)]; M. A. Braun and V. V. Vechernin, Yad. Fiz. **25**, 1276 (1977) [Sov. J. Nucl. Phys. **25**, 676 (1977)].
[70] L. P. Kaptar', B. L. Reznik, and A. I. Titov, Yad. Fiz. **42**, 777 (1985) [Sov. J. Nucl. Phys. **42**, 492 (1985)].
[71] J. R. Johnson, R. Kammerud, T. Ohsugi *et al.*, Phys. Rev. D **17**, 1292 (1978).
[72] A. Brenner, D. C. Carey, J. E. Elias *et al.*, Phys. Rev. D **26**, 1497 (1982).
[73] A. M. Baldin, V. K. Bondarev, N. Giordanescu *et al.*, Preprint E1-82-472, JINR, Dubna (1982).
[74] F. E. Taylor, D. C. Carey, J. R. Johnson *et al.*, Phys. Rev. D **14**, 1217 (1976).
[75] A. M. Baldin, Yu. A. Panebrattsev, and V. S. Stavinskiĭ, Preprint 1-84-185 [in Russian], JINR, Dubna (1984).
[76] A. M. Baldin, V. G. Grishin, L. A. Didenko *et al.*, in *Proc. of the Seventh International Seminar on Problems of High Energy Physics*, Vol. 1, 2-84-599 [in Russian] (JINR, Dubna, 1984), p. 233.
[77] I. I. Bazhanskiĭ, L. P. Kaptar', B. L. Reznik *et al.*, in *Proc. of the Eighth International Seminar on Problems of High Energy Physics*, Vol. 1, 1, 2-86-668 [in Russian] (JINR, Dubna, 1987), p. 318.
[78] G. Miller, E. D. Bloom, G. Buschhorn *et al.*, Phys. Rev. D **5**, 528 (1972).

Translated by Julian B. Barbour